

The effect of extracorporeal shock wave therapy on neural and non-neural contributors to ankle joint resistance to imposed movement in patients with chronic muscle hypertonia

G. van der Jagt

Technische Universiteit Delft

Achilles  
Rehabilitation Device



# The effect of extracorporeal shock wave therapy on neural and non-neural contributors to ankle joint resistance to imposed movement in patients with chronic muscle hypertonia

by

**G. van der Jagt**

in partial fulfillment of the requirements for the degree of

**Master of Science**  
in Mechanical Engineering

at the Delft University of Technology,  
to be defended publicly on Thursday June 29, 2017 at 10:30 AM.

Student number: 4031628  
Supervisors: Dr. ir. A. C. Schouten  
Dr. ir. W. Mugge  
Thesis committee: Dr. ir. A. C. Schouten, TU Delft  
Dr. ir. W. Mugge, TU Delft  
Dr. ir. G. Smit, TU Delft

*This thesis is confidential and cannot be made public until June 29, 2017.*

An electronic version of this thesis is available at <http://repository.tudelft.nl/>.



# Preface

I would like to thank my TU Delft supervisors Alfred Schouten and Winfred Mugge for their support, supervision, guidance and discussions during all phases of my graduation project. I would like to thank Ruud Selles and Ruud van der Veen from the Erasmus MC for their support, supervision and clinical guidance in and around the hospital environment. I would also like to thank Jurriaan de Groot from the LUMC for his insights and discussion on the neuromuscular model. Finally, I want to thank my family and friends for the moral support throughout my whole study, especially during the final phases of my graduation project.

*G. van der Jagt  
Delft, June 2017*



# The effect of extracorporeal shock wave therapy on neural and non-neural contributors to ankle joint resistance to imposed movement in patients with chronic muscle hypertonia

G. van der Jagt<sup>a,\*</sup>

<sup>a</sup>Faculty of Mechanical Engineering, Delft University of Technology, Delft, The Netherlands

---

## Abstract

**Introduction.** Increased joint resistance to imposed movement (“muscle hypertonia”) is a common finding in patients with an upper motor neuron syndrome, following stroke. Contributors to muscle hypertonia are of neural (increased reflex activity) and non-neural (altered visco-elastic properties) nature. Extracorporeal shock wave therapy (ESWT), a new noninvasive treatment modality, appears to be beneficial as hypertonia relieving therapy. However, clinical assessment such as the Ashworth test are unable to discriminate between underlying intrinsic and neural properties. Therefore, the effect of ESWT on the underlying neuromechanical components of muscle hypertonia remains unknown. The effect of ESWT on the contributors to joint resistance can be quantified using motorized ramp-and-hold movements and neuromuscular modeling of the musculoskeletal system of the ankle joint.

**Methods.** Patients with chronic muscle hypertonia ( $MAS > 1$ ) were measured using ramp-and-hold rotations applied by a robotic manipulator, using slow ( $15^\circ/s$ ) and fast ( $100^\circ/s$ ) movement velocities. Ankle angle, torque and EMG of the tibialis anterior, soleus, gastrocnemius medialis and lateralis were measured and used to fit a neuromuscular model to the measured joint resistance. The neuromuscular model contains 15 optimizable parameters which represent the intrinsic and active muscle components. Outcome measures were the estimated model parameters, the range of motion (ROM), and modified Ashworth scale (MAS) of the ankle joint.

**Results.** No effect of ESWT treatment was observed on the estimated model parameters and the passive ROM. The MAS was significantly lower after ESWT treatment ( $Z = -2.121$ ,  $p = 0.034$ ). Movement velocity introduced changes in the estimated model parameters.

**Conclusion.** Conflicting results between the biomechanical assessment (estimated model parameters, ROM) and clinical assessment (Ashworth test), raises questions about the validity of the Ashworth test. Furthermore, since no effect was observed on the neuromuscular model parameters, no conclusion can be drawn on the effect of ESWT on the neural and non-neural contributors to ankle joint resistance in patients with chronic muscle hypertonia.

**Keywords:** Stroke, Muscle hypertonia, Spasticity, Neuromuscular modeling, Biomechanical assessment

---

## 1. Introduction

Movement disorders—resulting from lesions to the central nervous system, as in stroke, multiple sclerosis, spinal cord injury, and traumatic brain injury—are characterized by increased joint resistance to im-

posed movement [1]. This increase in resistance is clinically referred to as “hypertonia”, or “muscle hypertonia” and is the cause of both neural and non-neural components, as a result of the upper motor neuron syndrome (UMNS). One of the main components contributing to hypertonia is spasticity which is defined by Lance (1980) as a neurological disorder characterized by a velocity-dependent increase in resistance to passive stretch and exaggerated tendon jerks, resulting from hyperexcitability of the stretch reflex, as one component of

---

\*Corresponding author  
Email address: G.vanderjagt@student.tudelft.nl (G. van der Jagt)

the UMNS [2]. Other symptoms of the UMNS include flexor spasms and loss of muscle strength and motor control. Together, these aspects of the UMNS may lead to intrinsic changes (altered tissue visco-elastic properties, i.e. contractures, fibrosis, atrophy) to the underlying muscle and joint tissue which reflect the non-neural components of hypertonia [1]. Besides the increased resistance, joints may also suffer from a reduced passive range of motion (ROM) [3]. Together, these impairments may introduce abnormal posture of the patient and seriously interfere with patients' function in mobility, comfort and many activities of daily living, and may include pain [3, 4]. It is therefore important that proper assessment and treatment be provided to patients with muscle hypertonia.

Current hypertonia reducing treatment consists of physical therapy, oral medication using agents such as baclofen, tizanidine, benzodiazepines, dantrolene and gabapentin, and chemical nerve blocks using phenol and botulinum toxin injection [5]. However, physical therapy is partially ineffective due to the reoccurring effect of spasticity during the chronic phase. Antispasticity drugs are partially ineffective since they only affect the neural components of muscle hypertonia. Furthermore, pharmacological treatment may show side effects, and the regrowth of nerve connections may reduce the efficacy of chemical nerve blocks [5]. For these reasons, it may be beneficial for future treatment to take other noninvasive methods into considerations.

Extracorporeal shock wave therapy (ESWT) is a widely used noninvasive treatment modality in various musculoskeletal disorders including proximal plantar fasciitis of the heel, lateral epicondylitis of the elbow, calcific tendinitis of the shoulder and non-union of long bone fracture [6]. ESWT makes use of high-energy shock waves which are generated outside the body, and are then directed into biological tissue using an ultrasound gel as a coupling agent. Shock waves can be represented by a pressure wave consisting of a repeating pattern of high- and low-pressure regions moving through a compressible medium. Clinically applied shock waves move through biological tissue by alternating expansion and compression of the tissue, causing changes in the local tissue pressure (relative to the ambient pressure) along the direction of propagation [7]. These changes in local pressure result in two types of mechanical forces acting on the biological tissue. One represents the direct generation of mechanical forces onto the biological tissue. The second represents secondary forces due to the formation of cavitation bubbles during the low tensile pressure phase of the shock wave [7].

Recently, ESWT is also reported to be beneficial as hypertonia relieving therapy in patients affected by stroke [8–15] and cerebral palsy [16–18]. During clinical practises, the severity of muscle hypertonia is assessed using the Modified Ashworth Scale (MAS). The MAS is a clinical score that measures the resistance to passive stretch as felt by the examiner during a passive, one second joint rotation over its full ROM [19, 20]. The MAS grades muscle hypertonia according to six ordinal levels:

- 0 Normal muscle tone
- 1 Slight increase in muscle tone, manifested by a catch and release or by minimal resistance at the end of the range of motion when the affected part(s) is moved in flexion or extension
- 1+ Slight increase in muscle tone, manifested by a catch, followed by minimal resistance throughout the remainder (less than half) of the ROM
- 2 More marked increase in muscle tone through most of the ROM, but affected part(s) easily moved
- 3 Considerable increase in muscle tone, passive movement difficult
- 4 Affected part(s) rigid in flexion or extension

For example, Manganotti et al. (2005) studied the effect of a single ESWT session compared to placebo in patients with upper limb hypertonia. They found a significant effect of ESWT on the MAS directly after treatment, which lasted up to 4 weeks [8]. Alongside the positive effects on the MAS, some studies reported that ESWT had no significant effect on spinal excitability and nerve damage [8, 10, 21]. Another common measure that is used to assess the severity of muscle hypertonia is the ROM. The ROM is defined as difference between the maximum flexion and extension angles that the joint in question is able to reach, while the patient is in rest (that is, no voluntary muscle contraction). In clinical practises, the ROM is expressed in degrees and is often measured by the examiner using a goniometer. Several studies studied the effect of ESWT on the ROM in patients with chronic muscle hypertonia. They found a significant increase of the ROM directly after ESWT, which sometimes lasted up to 4 weeks [8, 9, 11, 15, 16, 18, 21].

However, despite being the golden standard for assessing muscle hypertonia, the MAS has some major flaws: it is a subjective tool that grades hypertonia on an ordinal scale, which limits its accuracy and reliability. Furthermore, the MAS is unable to discriminate between the neural and non-neural contributors to muscle hypertonia. Therefore, despite the positive results on the

MAS, the effect of ESWT on the underlying biomechanical properties of muscle hypertonia remains unknown.

In recent studies, a new method was developed to successfully estimate neural and non-neural contributors to muscle hypertonia in patients with stroke [22, 23] and cerebral palsy (CP) [24, 25]. The method makes use of motorized assessment in combination with neuromuscular modeling to investigate the individual components of the total joint resistance. First, a robotic manipulator was used to experimentally obtain the total joint resistance (mechanically represented by torque about the joint) during imposed ramp-and-hold (RaH) movement over the full ROM. Measured data was then used to obtain physiological interpretable parameters by fitting a nonlinear neuromuscular model to the measured joint torque. The validated model yielded quantitative parameters that represent the intrinsic (non-neural) and active (neural) muscle components of the total joint torque [22–25].

The main goal of this study was to objectively quantify the effects of a single ESWT session on neural and non-neural contributors to ankle joint resistance in patients with chronic muscle hypertonia, using motorized assessment in combination with neuromuscular modeling of the ankle joint. Since spasticity—one of the components of muscle hypertonia—is said to be velocity dependent [2], the effect of movement velocity on the physiological parameters was also tested. The secondary objective of this study was to evaluate if we can replicate the positive outcomes from literature of the efficacy of ESWT on the ROM and MAS. It was hypothesized that ESWT lowers joint resistance by directly acting on the intrinsic components (i.e. fibrosis) of chronic muscle hypertonia [8, 15, 17]. In the current study, this would be reflected in the outcome measures as a significant change in the estimated parameters that describe the intrinsic part of the neuromuscular model. Furthermore, we hypothesized an increase in ROM and a decrease on the MAS grade directly after a single ESWT session in patients with chronic muscle hypertonia.

Increased knowledge of the effects of ESWT on the underlying neuromechanical parameters of muscle hypertonia may help design patient-specific treatment protocols.

## 2. Methods

### 2.1. Subjects

Nine patients with chronic muscle hypertonia with MAS > 1 (mean age 45.2 years, SD 16.2 years) were recruited from the Department of Rehabilitation Medicine

of the Erasmus University Medical Center and the Rijn- dam Rehabilitation Center, Rotterdam, the Netherlands. Inclusion criteria were patients with stable spasticity (no variability on the MAS within two months before recruitment) in the lower extremity (at least grade 1+ measured by the MAS) at least nine months after the onset of the cerebral vascular incident or traumatic brain injury to reduce the confounding effect of natural recovery. Patients with fixed contractures of the ankle, or prior botulinum toxin treatment within the six months preceding the study were excluded. The study was approved by the local ethics committee of the Erasmus University Medical Center. All participants gave their written informed consent prior to the experiment. An overview of the patient demographics is shown in Table 1.

### 2.2. Instrumentation

Subjects were comfortably seated with their hip and knee positioned both in approximately 70° flexion, determined by goniometry. The foot of the most affected leg was fixed in a footplate using Velcro straps. Ankle rotations were applied by the Achilles Rehabilitation Device (MOOG, Nieuw Venneep, The Netherlands), a single horizontal axis powered footplate (Figure 1). Axes of the ankle and motor were aligned by visually minimizing knee translation in the sagittal plane while rotating the ankle.

Muscle activity of the ankle dorsiflexor, tibialis anterior (TA); and plantar flexors, soleus (SOL), gastrocnemius medialis (GM) and gastrocnemius lateralis (GL) were measured by bipolar surface electromyography (EMG) using a Porti system (TMSi B.V., The Netherlands). Inter electrode distance was 20 mm. A ground electrode was placed on the patella of the subject, and served to keep subject potential and amplifier potential at the same level. The EMG signals were pre-amplified (gain = 20), and filtered with a 1st order low-pass filter (signal anti-aliasing), before being sampled at 1000 Hz. Each recorded signal was then high-pass filtered (bi-directional 3rd order Butterworth at 20 Hz), rectified and low-pass filtered (uni-directional 4th order Bessel filter at 20 Hz) to obtain the envelope. Due to technical difficulties of the Porti system, a second Porti system (TMSi B.V., The Netherlands) was used as backup, which measured the muscle activity at a sample rate of 1024 Hz. The minimal EMG value (determined over a 125 samples window (125 ms) and moved with steps of 8 samples (8 ms) over the whole signal) was subtracted from the total EMG to eliminate any background muscle activity. Ankle torque and joint angle were recorded by the Achilles at a sample frequency of 1024 Hz. To prevent amplification of the noise due to differentiation,

**Table 1:** Subject demographics

ID	Age (years)	Gender	Diagnosis	Post incident (months)	Affected side	MAS
1	45	M	CVA	16	Left	2
2	54	M	CVA	22	Right	3
3	32	F	TBI	103	Right	2
4	21	F	CVA	17	Left	1+ <sup>a</sup>
5	34	F	CP	410 <sup>b</sup>	Right	3
6	70	F	CVA	56	Right	3
7	35	F	CVA	25	Right	3
8	65	M	CVA	151	Left	2
9	51	M	CVA	134	Left	3

Note.—MAS = Modified Ashworth Scale; CVA = cerebrovascular accident; TBI = traumatic brain injury; CP = cerebral palsy.

<sup>a</sup> Value on the modified Ashworth scale, between 1 and 2.

<sup>b</sup> Incident at birth.



**Figure 1:** Measurement setup of the Achilles Rehabilitation Device (MOOG, Nieuw Venneep, The Netherlands).

torque and angle signals were filtered with the same 4th order low-pass filter at 20 Hz. All data was re-sampled by a factor 8 (125 Hz and 128 Hz respectively).

### 2.3. Treatment protocol

ESWT was performed while the subject remained seated in the measurement setup. ESWT was performed by an ESWT-certified physical therapist using the Swiss DolorClast<sup>®</sup> Master (EMS, Nyon, Switzerland) using a 15 mm applicator attached to the EvoBlue handpiece. The point of the ESWT site is placed at the muscle belly of the plantar flexor muscles. Each subject received one session of ESWT that comprises 3000 pulses (1000 per

muscle belly: SOL, GM, and GL) at a frequency of 8 Hz. The energy level was set at 2.0 bar. The probe was oriented perpendicular to the subject's calf muscles, using ultrasound gel as coupling agent.

### 2.4. Measurement protocol

Measurements were performed on the most affected leg of each patient. Before the measurement, the foot was manually rotated until the subjects noted their limit of comfort in both dorsiflexion and plantar flexion. As a safety measure, two physical pins were inserted in the motor to physically block the motor from rotating out of this comfort range. Subsequently, the foot was po-

sitioned at an initial angle of  $15^\circ$  plantar flexion, determined by goniometry. The ankle angle was defined as the position of the foot with respect to the lower leg, where the perpendicular (neutral) position was defined as zero degrees. Rotation in dorsiflexion was defined to be positive. Maximum dorsiflexion angle was determined by a gradually increasing torque imposed by the manipulator from zero to a maximum of 15 Nm (dorsiflexion torque). Maximum plantar flexion angle was determined in a similar fashion, with a gradually decreasing torque from zero to a minimum of  $-7.5$  Nm (plantar flexion torque). These boundaries were chosen such that they stayed within the comfort region of patients with chronic muscle hypertonia. Torques higher than 15 Nm or lower than  $-7.5$  Nm typically resulted in discomfort of the patients. The ROM was defined as the difference between the maximum dorsiflexion and plantar flexion angle and was used as the boundary for the subsequent RaH rotations.

RaH rotations were performed by the Achilles manipulator through the full ROM at angular velocities of  $15^\circ/\text{s}$  and  $100^\circ/\text{s}$ , referred to as *slow* and *fast* trials respectively. Prior to each RaH rotation, the foot was rotated from its initial position to the maximum plantar flexion angle in 2 s time. After a random delay of 4 s to 5 s, the foot was rotated to the maximum dorsiflexion angle with a constant velocity. The hold phase had a random duration of 4 s to 5 s, after which the foot was rotated back to the maximum plantar flexion angle with the same constant velocity. After each RaH rotation, the foot was moved back to its initial position. Time to cover a complete RaH rotation did not exceed 25 s. Rest periods of about 30 s were introduced between each RaH rotation to reduce possible thixotropic effects. Each RaH rotation was performed twice to test for repeatability of the estimation procedure, resulting in a total of 1 ROM and 4 RaH (two slow and two fast) trials per measurement session. RaH rotation profiles were provided in a pseudo-random order (with a total of six possibilities; e.g. slow-slow-fast-fast, or slow-fast-fast-slow, with each possibility occurring once for every six subjects) to eliminate possible effects of trial order. Each subject received two measurement sessions; one before (*pre*) and one directly after (*post*) ESWT was applied, resulting in a total of 2 ROM and 8 RaH rotations per subject. Subjects were instructed to remain relaxed and not actively resist any motions during the entire experiment.

For clinical testing, the MAS was used to assess muscle hypertonia of the ankle plantar flexor: triceps surae (TS: SOL, GM, GL). The MAS was measured directly before (*pre*) and directly after (*post*) ESWT was ap-

plied. To limit the interference with the biomechanical measurements, the clinical measurements were performed directly before and directly after all biomechanical measurements, resulting in the following order of assessment: pre-MAS, pre-biomechanical, ESWT, post-biomechanical and post-MAS. Clinical testing was performed by an experienced physical therapist who was instructed to perform the Ashworth test as he would perform normally in clinic, to avoid obtaining biased and study-specific results.

## 2.5. Neuromuscular model

Measured signals of the RaH rotations were used to obtain physiological interpretable parameters by fitting a nonlinear neuromusculoskeletal model of the ankle joint to the measured ankle torque. The model was previously described by de Vlugt et al. [22], and has had a few alterations over the years [23–25]. The model takes measured ankle angle and muscle EMG as input and estimates the total ankle torque by optimizing 15 physiological interpretable parameters: 7 that represent the intrinsic muscle (*non-neural*) components, and 8 that represent the active muscle (*neural*) components. The intrinsic parameters describe the passive forces around the ankle joint. Here, the mass of the foot and footplate are lumped together into one mass  $m$ , and is used to compute the inertial and gravitational forces around the ankle joint. Visco-elastic properties of the muscles are represented by a spring system which describes the resistance of the parallel connective tissue (stiffness coefficients  $k_{ts}$  and  $k_{ta}$ ) as a result of stretching the muscles beyond their slack lengths ( $x_{0,ts}$  and  $x_{0,ta}$ ). When muscle connective tissue is under continuous tension, its elastic force will decrease over time. This decrease in elastic muscle force is attributed to muscle relaxation dynamics [26–28], which is modeled by a first order filter (relaxation time constant  $\tau_{rel}$ , relaxation factor  $k_{rel}$ ). The active muscle parameters describe the force of the muscles during active contraction, based on the Hill-type muscle model, including: EMG weighting factors ( $g_1 - g_4$  for the TA, SOL, GM and GL respectively), optimal muscle lengths ( $l_{0,ts}$  and  $l_{0,ta}$ ), and second-order activation dynamics (cut-off frequency  $f_0$ , damping factor  $\beta$ ). The muscle tendons were assumed to be infinitely stiff. Model parameters were defined on the linear muscle level. An overview of the model parameters is shown in Table 2.

The total modeled joint torque is described as a summation of the inertial torque, gravitational torque, and muscle torques, described as:

$$T_{\text{mod}}(t) = I\ddot{\theta}(t) + T_{\text{grav}}(\theta) + T_{ts}(t) - T_{ta}(t) \quad (1)$$

**Table 2:** Model parameters, including their initial and boundary values for parameter estimation

Parameter	Unit	Description	Initial	LB	UB
<i>Non-neural</i>					
$m$	kg	Mass (foot + footplate)	1.5	1.2	3.0
$k_{ts}$	1/m	Stiffness coefficient TS	200	10	600
$k_{ta}$	1/m	Stiffness coefficient TA	200	10	600
$x_{0,ts}$	m	Muscle slack length TS	0.05	0.01	0.09
$x_{0,ta}$	m	Muscle slack length TA	0.05	0.01	0.11
$\tau_{rel}$	s	Tissue relaxation time constant	2	0.1	6
$k_{rel}$	-	Tissue relaxation factor	0.1	0.05	3
<i>Neural</i>					
$g_1$	1/V	EMG weighting factor TA	$1 \times 10^4$	1	$1 \times 10^{10}$
$g_2$	1/V	EMG weighting factor SOL	$1 \times 10^4$	1	$1 \times 10^{10}$
$g_3$	1/V	EMG weighting factor GM	$1 \times 10^4$	1	$1 \times 10^{10}$
$g_4$	1/V	EMG weighting factor GL	$1 \times 10^4$	1	$1 \times 10^{10}$
$l_{0,ts}$	m	Optimal muscle length TS	0.048	0.02	0.09
$l_{0,ta}$	m	Optimal muscle length TA	0.068	0.02	0.11
$f_0$	Hz	Activation cut-off frequency	2	0.05	4
$\beta$	-	Activation damping factor	1	0.1	1.5

Note.—LB = lower bound; UB = upper bound; TS = triceps surae; TA = tibialis anterior; SOL = soleus; GM = gastrocnemius medialis; GL = gastrocnemius lateralis.

where  $t$  represents the independent time variable,  $T_{mod}(t)$  the modeled ankle reaction torque,  $\theta(t)$  the measured ankle joint angle,  $\ddot{\theta}(t)$  the ankle joint angular acceleration,  $I$  the inertia of the ankle plus footplate,  $T_{grav}(\theta)$  the torque due to gravitation,  $T_{ts}(t)$  the torque generated by the TS, and  $T_{ta}(t)$  the torque generated by the TA. Note that the torque generated by the TA is subtracted from the total, as its forces result in a torque around the ankle joint in opposite direction (compared to those of the TS). Muscle torques for the plantar flexion and dorsiflexion muscles can be broken down in passive-elastic (*non-neural*) and active (*neural*) components, described as:

$$\begin{aligned} T_m(t) &= (F_{elas,m}(t) + F_{act,m}(t)) r_m(\theta) \\ &= T_{elas,m}(t) + T_{act,m} \end{aligned} \quad (2)$$

where  $m$  represents the muscle group (TS and TA),  $F_{elas,m}(t)$  the elastic force of the parallel connective tissue,  $F_{act,m}(t)$  the active muscle force according to the Hill-type muscle model,  $r_m(\theta)$  the angle dependent moment arm of the muscle tendon,  $T_{elas,m}(t)$  the elastic torque, and  $T_{act,m}(t)$  the active muscle torque. Combin-

ing Equation (1) and Equation (2) together gives:

$$\begin{aligned} T_{mod}(t) &= \underbrace{I\ddot{\theta}(t) + T_{grav}(\theta) + T_{elas,ts}(t) - T_{elas,ta}(t)}_{\text{non-neural}} \\ &\quad + \underbrace{T_{act,ts}(t) - T_{act,ta}(t)}_{\text{neural}} \end{aligned} \quad (3)$$

A full description of the model and its derivation is shown in Appendix A.

## 2.6. Parameter estimation

Parameter estimation was done in time domain by fitting the model from Equation (3) on top of the measured ankle torque. Recorded signals were cut to start 2 s before the start of the first ramp to eliminate possible start-up effects. As fit criterion, the sum of the quadratic difference between the measured and modeled torque was minimized over all time samples and all trials, fitting all parameters in one optimization per subject, described as:

$$e(t) = T_{meas}(t) - T_{mod}(t) \quad (4)$$

$$E = \sum_{j=1}^k \sum_{i=1}^N e_{i,j}^2(t) \quad (5)$$

where  $e(t)$  represents the error vector between the measured torque  $T_{meas}(t)$  and the modeled torque  $T_{mod}(t)$ ,  $E$  the total value of the fit criterion,  $i$  indexes the time

vector (with  $N$  total samples), and  $j$  indexes the trial number (with  $k$  total trials). The parameter estimation process is visualized in Figure 2. The model consists of fifteen model parameters which were estimated for each RaH trial, guided by parameter boundaries to prevent unrealistic parameter values and bad convergence (see Table 2). Ten of these parameters were estimated for each trial separately (condition dependent parameters), whereas the mass  $m$  and EMG weighting factors  $g_1 - g_4$  were shared between trials of the same subject, as they were not expected to change between different RaH rotations (condition independent parameters). The error vector  $e(t)$  was summed over all time samples and all trials for each subject. Ten parameters were estimated for each of the eight trials and five parameters were shared between trials of the same subject, resulting in a total of 85 parameters for each subject. Estimated model parameters were then averaged over each repeated trial, resulting in a total of four sets of parameters per subject under the following conditions: pre-ESWT: slow and fast; post-ESWT: slow and fast. Parameter and model estimation and analysis were performed in Matlab R2016b (The Mathworks Inc., Natick MA).

### 2.7. Model validity and parameter accuracy

Model internal validity was assessed by computing the Variance Accounted For (VAF, “goodness of the fit”) [22–25]. The VAF relates how much of the variance in the measured data can be explained by the model, described as:

$$VAF = \left( 1 - \frac{\sum (T_{\text{meas}}(t) - T_{\text{mod}}(t))^2}{\sum (T_{\text{meas}}(t))^2} \right) 100\% \quad (6)$$

where  $T_{\text{meas}}(t)$  represents the measured torque, and  $T_{\text{mod}}(t)$  the modeled torque. However, the VAF as described in Equation (6) is defined only for signals with a mean value of zero. In order to account for this drawback, the VAF was computed by subtracting the mean from the signals, described as:

$$VAF = \left( 1 - \frac{\sum (T_{\text{meas}}^*(t) - T_{\text{mod}}^*(t))^2}{\sum (T_{\text{meas}}^*(t))^2} \right) 100\% \quad (7)$$

where  $T_{\text{meas}}^*(t)$  and  $T_{\text{mod}}^*(t)$  represent the measured and modeled torque, corrected by their mean values, according to:

$$T_{\text{meas}}^*(t) = T_{\text{meas}}(t) - T_{\text{mean}}(t) \quad (8)$$

$$T_{\text{mod}}^*(t) = T_{\text{mod}}(t) - T_{\text{mean}}(t) \quad (9)$$

$$T_{\text{mean}}(t) = \frac{T_{\text{meas}}(t) + T_{\text{mod}}(t)}{2} \quad (10)$$

The VAF for the modeled torque was calculated for each trial. A VAF of 100 % means that the measured data is perfectly described by the model.

Parameter accuracy was examined by computing the standard error of the mean (SEM) of the estimated model parameters. The SEM is described as:

$$SEM = \sqrt{\frac{1}{N} \text{diag}(J^T J)^{-1} e(t)^T e(t)} \quad (11)$$

where  $N$  is the number of time samples,  $J$  the Jacobian matrix, and  $e(t)$  the error vector between the measured and modeled torque. Low SEM values (compared to their corresponding parameter value) indicate high sensitivity of the modeled parameter. High sensitivity means that the parameter has a considerable contribution to the modeled output torque, and therefore indicates that the parameter is not redundant [22, 29]. For visual analysis, SEM values were normalized to their corresponding parameter values.

### 2.8. Statistical analysis

To test the effect of ESWT on the ROM within-subjects, a paired-samples t-test was used. To test the effects of ESWT and movement velocity on the model parameters within-subjects, a two-way repeated measures ANOVA was used with Bonferroni correction. For the two independent factors, *ESWT* (two levels: pre and post) and *velocity* (two levels: slow and fast) were used. Inter-trial repeatability of the parameter estimates between repeated trials with the same conditions was examined using the intraclass correlation coefficients (ICC, 2-way mixed model). To test the effect of ESWT on the MAS within-subjects, a Wilcoxon signed rank test was used. This test was used to determine whether there is a median difference in rank of the MAS after ESWT. For statistical purposes, a MAS score of 0 was linked to rank 0; a MAS score of 1+ to rank 1; a MAS score of 2 to rank 3; and so on (similar to [10, 13, 21]). Statistical analysis was performed using IBM SPSS Statistics 24.0 (IBM Corp., Armonk NY) with an alpha value of 0.05.

## 3. Results

### 3.1. Measured data

All subjects were able to comply with the protocol. Figure 3 shows an example of measured data, including imposed RaH movement profiles (Figure 3: A-B), corresponding joint torques (Figure 3: C-D) and muscle activity (Figure 3: E-L) for a typical subject with MAS grade of 3. The example shows data for one slow (left

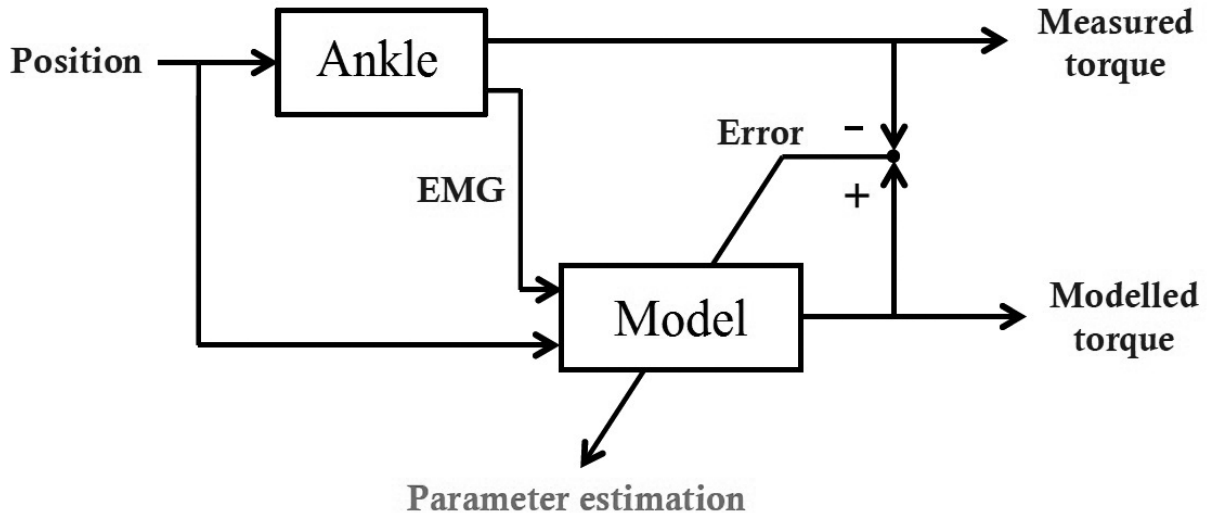


**Figure 2:** Schematic representation of the parameter estimation process. The Achilles Rehabilitation Device imposes RaH rotations (*position*) to the subject’s ankle. As a result, the subject exerts a resisting torque which is measured by the Achilles. Simultaneously, subject’s muscle activity is recorded by bipolar surface EMG. Position and EMG signals are then used as input to a neuromuscular model of the ankle, which simulates the ankle resistance as described in Appendix A. The error between the modeled and measured torque is then minimized by estimating 15 model parameters (see Table 2), using a least-squares algorithm.

column) and one fast (right column) trial, both measured before ESWT was performed. A typical torque profile consists of a quick increase in torque at the start of the ramp phase. When the torque approaches 0 Nm, the rate with which the torque increases slows down. This is shown as a “flattening” in the torque profile during the ramp phase. At this point, the ankle reaches its neutral angle: the angle for which the resulting joint torque equals zero. After the neutral angle has been passed, the torque increases exponentially, reaching a peak value near the end of the first ramp phase. This is shown in the example data at a time instant of  $\sim 5$  s for the slow trial (see Figure 3: C), and at  $\sim 2.5$  s for the fast trial (see Figure 3: D). During the fast trials, this peak is often assisted by an increase in muscle activity, which further increases the peak value. Muscle activity is most dominant for the SOL muscle during the fast trials (see Figure 3: H). When the movement has stopped at the maximum dorsiflexion angle, the torque slowly decays to a value that is independent of time. During this phase, the TS muscles are under continued tension, resulting in a relaxation or force decrease from these muscles [26–28]. This phenomenon is modeled by a first order filter as described in Appendix A. After the hold phase, the movement goes back to the maximum plantar flexion angle. During this rotation, the TA muscle is being stretched, whereas the TS muscles are being shortened. The movement passes through the neutral angle again,

after which it comes to a full stop at the maximum plantar flexion angle. The torque reaches a negative peak at the end of the second ramp phase, resulting from the maximally stretched TA muscle.

Typical EMG profiles show larger muscle activity (higher magnitude) during the fast trials, compared to the slow trials (see Figure 3: E-L). This is to be expected since reflex activity is known to be velocity dependent: faster movement results in a stronger reflex activity. Muscle activity for the TS muscles is larger compared to the activity of the TA (see Figure 3: F, H, J, L). Among all muscles, the SOL showed the largest activity in response to the RaH movement. It was shown by Sloot et al. (2015) that the joint resistance in the  $70^\circ$  knee flexion position was almost fully described by the SOL muscle, since the two gastrocnemii GM and GL are in a shortened state, compared to a stretched leg with knee flexion of  $20^\circ$  [25]. As a result, contributions of the SOL are expected to be larger than contributions of the GM and GL in a position with knee flexion of  $70^\circ$ . The muscle activity of the TS muscles emerged in brief bursts, which slowly decayed in magnitude over time, possibly representing the occurrence of a clonus in the calf muscles.

Measured data for each subject is shown in Appendix B.

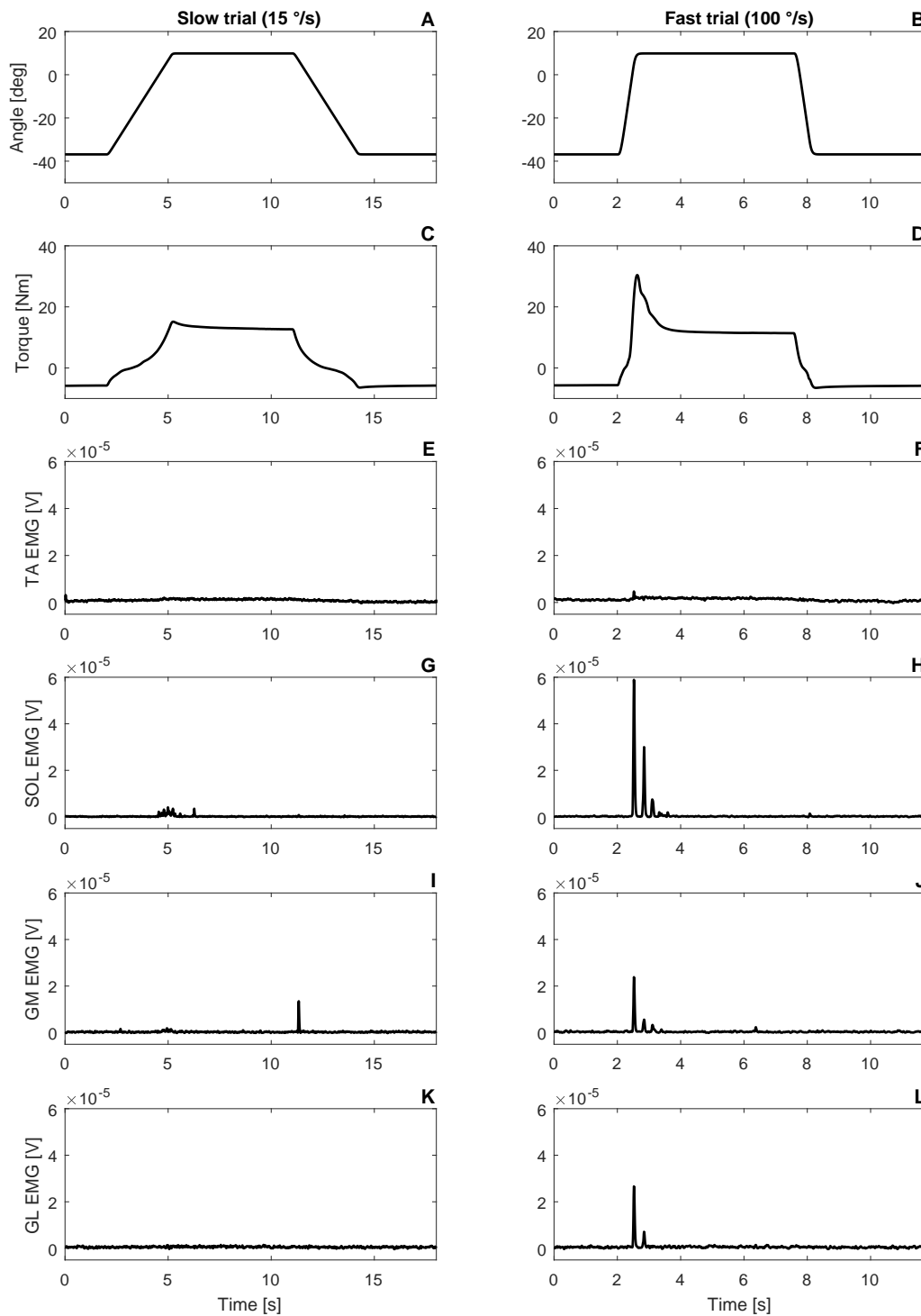


**Figure 3:** Example of imposed ramp-and-hold (RaH) movement profiles, joint torques and muscle EMG, for a typical subject with MAS grade of 3 (measured before ESWT). Left column: slow trial. Right column: fast trial. A-B: imposed RaH rotation on the ankle; C-D: measured joint torque; E-F: EMG from the tibialis anterior (TA); G-H: EMG from the soleus (SOL); I-J: EMG from the gastrocnemius medialis (GM); K-L: EMG from the gastrocnemius laterals (GL).

### 3.2. Modeled data

All RaH trials were used to simulate the model torque, and estimate model parameters. Figure 4 shows an example of measured torque (grey traces) together with modeled torque fits (black traces) for a typical subject with MAS grade of 3. The data shown in Figure 4 are from the same subject and same trials as in Figure 3. Rows from top to bottom show imposed RaH movement profiles (Figure 4: A-B), corresponding measured (grey) and modeled (black) torque (Figure 4: C-D), passive-elastic muscle torques (Figure 4: E-F), active muscle torques (Figure 4: G-H), and inertial and gravitational torques (Figure 4: I-J). VAF values for these model fits were 99.9% and 99.4% for the slow and fast trial respectively.

Typically at the start of each trial, when the foot is in its maximum plantar flexion angle, the elastic torque of the TS equals zero and increases exponentially during the first ramp phase (see Figure 4: E-F). After the movement has come to a full stop at the maximum dorsiflexion angle, the elastic torque of the TS slowly decreases due to relaxation of the muscles. This takes less than half a second, after which the elastic torque is sustained at a constant level. During the second ramp phase, the elastic torque decreases rapidly until it reaches zero, which completes the trial. The TA shows similar behavior, but in opposite direction: when the elastic torque of the TS increases, the elastic torque of the TA decreases, and vice versa (see Figure 4: E-F).

EMG activity was typically observed in the TS during the first ramp phase of the fast trials, generally consisting of one or several peaks (see Figure 3: H, J, L). This EMG activity resulted in active muscle torques, which persisted for about 1 s to 2 s due to the activation dynamics of the muscles (see Figure 4: H). EMG during the slow trials was generally absent, resulting in minimal to no active muscle torques during the slow trials (see Figure 4: G).

### 3.3. Parameter estimates

The ten condition-dependent parameters (stiffness coefficients  $k_{ts}$  and  $k_{ta}$ , muscle slack lengths  $x_{0,ts}$  and  $x_{0,ta}$ , tissue relaxation time constant  $\tau_{rel}$  and factor  $k_{rel}$ , optimal muscle lengths  $l_{0,ts}$  and  $l_{0,ta}$ , and activation cut-off frequency  $f_0$  and damping factor  $\beta$ ) were estimated for each trial separately and are shown in Table 3 (mean  $\pm$  SD). The five condition-independent parameters (mass foot and footplate  $m$ , and EMG weighting factors  $g_1 - g_4$  for the TA, SOL, GM, and GL) were shared between trials within the same subject and are shown in Table 4 (mean  $\pm$  SD).

### 3.4. Model validity and parameter accuracy

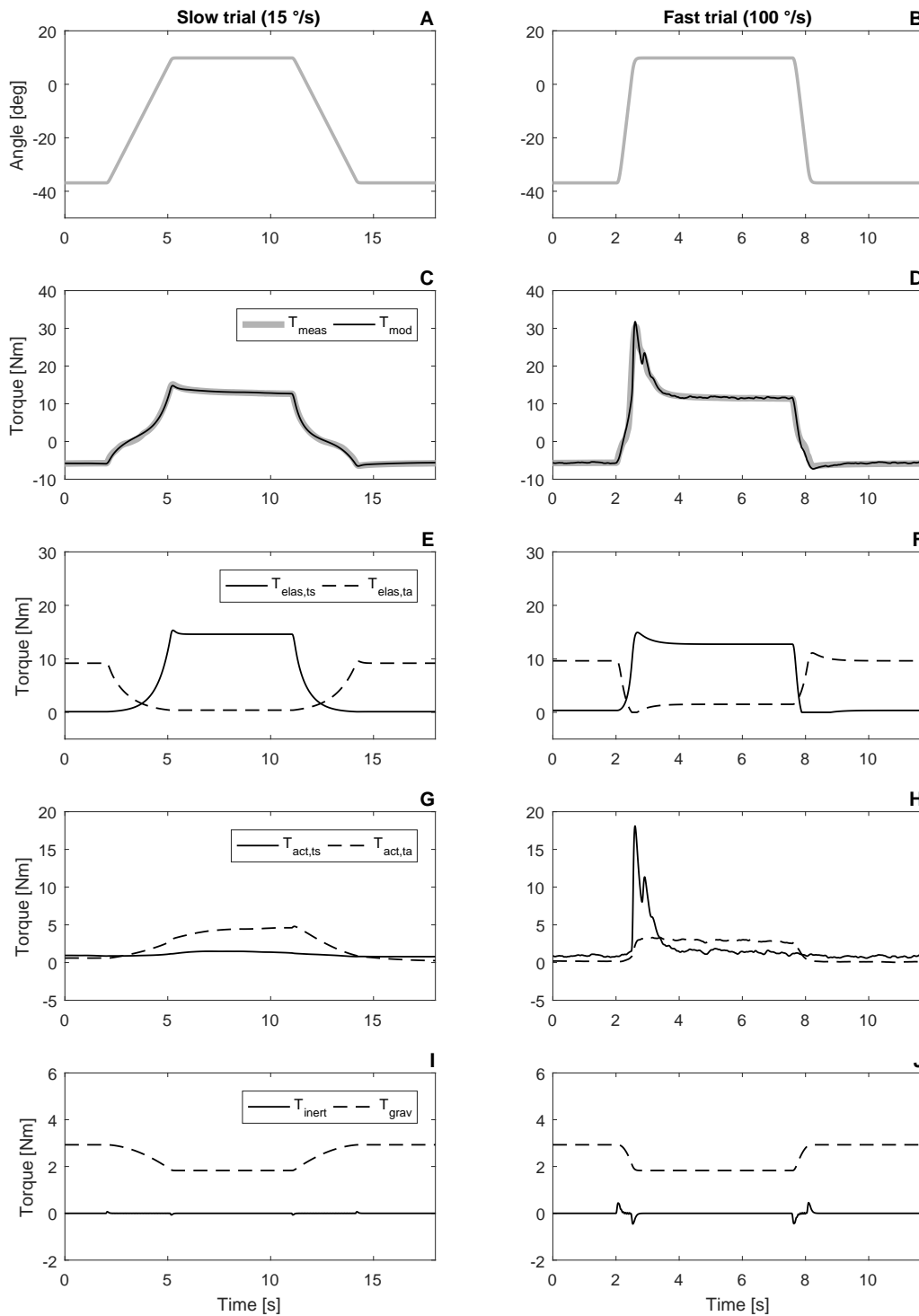
The VAFs between the measured and modeled torque were above 98% for all RaH trials, with a total average of 99.7%  $\pm$  0.4% (mean  $\pm$  SD). The slow trials had an average VAF of 99.9%  $\pm$  0.1%. The fast trials had an average VAF of 99.5%  $\pm$  0.5%. These high VAFs indicate that the measured ankle torque could be well described by the neuromuscular model. Model fits for each subject are shown in Appendix C.

Figure 5 shows the normalized SEM values for the ten condition-dependent parameters, separated for the slow and fast trials. Figure 6 shows the normalized SEM values for the five condition-independent parameters. On average, all SEM values were less than 35%, except for the weighting factors for the soleus ( $g_2$ ) and gastrocnemius medialis ( $g_3$ ). Extreme values in these weighting factors may be the result of redundancy in these parameters. For example, torque generated from active muscle contraction in the triceps surae is computed from its corresponding neural input. This neural input is a linear combination of the weighting factors and corresponding muscle EMG of the soleus and both gastrocnemii (see Equation (A.13)). As a result, only one of these weighting factors ( $g_2 - g_4$ ) may be sufficient to describe the active torque from the triceps surae. This goes paired with the fact that all three muscles of the TS show similar EMG behavior when they are being contracted (simultaneous contraction, see Figure 3: H, J, L).

Parameters of the muscle visco-elastic components (stiffness coefficients  $k_{ts}$  and  $k_{ta}$ , muscle slack lengths  $x_{0,ts}$  and  $x_{0,ta}$ , and tissue relaxation time constant  $\tau_{rel}$  and factor  $k_{rel}$ ) had a high accuracy for both the slow (median SEM < 5%) and fast trials (median SEM < 4%). Parameters of the neural components (optimal muscle lengths  $l_{0,ts}$  and  $l_{0,ta}$ , and activation cut-off frequency  $f_0$  and damping factor  $\beta$ ) were more accurate for the fast trials (median SEM < 8%) compared to the slow trials (median SEM < 24%). The inaccuracy of these parameters during slow trials may be the result of a lack of muscle activity (see Figure 3: E, G, I, K). With minimal to no muscle activity, contributions of the active muscle torques to the total modeled output torque is minimal, and may result in badly scaled parameters.

### 3.5. Repeatability

Inter-trial repeatability of the parameter estimates between repeated trials with the same conditions was moderate to good (ICC: 0.615 to 0.953), except for the optimal muscle length of the TA ( $l_{0,ta}$ ) (ICC: 0.357).



**Figure 4:** Example of model fit on top of measured torque data, for a typical subject with MAS grade of 3 (measured before ESWT). Left column: slow trial. Right column: fast trial. A-B: imposed RaH rotation on the ankle; C-D: measured joint torque (grey) and modeled torque (black); E-F: elastic muscle torques from the triceps surae (TS, solid) and tibialis anterior (TA, dashed); G-H: active muscle torques from the triceps surae (TS, solid) and tibialis anterior (TA, dashed); I-J: inertial (solid) and gravitational (dashed) torques.

**Table 3:** Condition-dependent model parameters

Parameter	Pre-ESWT (mean $\pm$ SD)		Post-ESWT (mean $\pm$ SD)	
	Slow	Fast	Slow	Fast
<i>Non-neural</i>				
Stiffness coefficient TS, $k_{ts}$ [1/m]	299 $\pm$ 39	269 $\pm$ 40	301 $\pm$ 59	261 $\pm$ 35
Stiffness coefficient TA, $k_{ta}$ [1/m]	198 $\pm$ 76	143 $\pm$ 64	180 $\pm$ 78	139 $\pm$ 66
Muscle slack length TS, $x_{0,ts}$ [m]	0.020 $\pm$ 0.003	0.018 $\pm$ 0.004	0.020 $\pm$ 0.003	0.017 $\pm$ 0.004
Muscle slack length TA, $x_{0,ta}$ [m]	0.064 $\pm$ 0.010	0.047 $\pm$ 0.020	0.060 $\pm$ 0.013	0.044 $\pm$ 0.024
Tissue relaxation time constant, $\tau_{rel}$ [s]	0.98 $\pm$ 0.82	1.67 $\pm$ 1.68	0.94 $\pm$ 0.89	1.39 $\pm$ 0.94
Tissue relaxation factor, $k_{rel}$ [–]	0.41 $\pm$ 0.21	0.66 $\pm$ 0.57	0.49 $\pm$ 0.32	0.71 $\pm$ 0.65
<i>Neural</i>				
Optimal muscle length TS, $l_{0,ts}$ [m]	0.083 $\pm$ 0.016	0.046 $\pm$ 0.016	0.081 $\pm$ 0.020	0.059 $\pm$ 0.023
Optimal muscle length TA, $l_{0,ta}$ [m]	0.074 $\pm$ 0.025	0.060 $\pm$ 0.035	0.065 $\pm$ 0.030	0.045 $\pm$ 0.022
Activation cut-off frequency, $f_0$ [Hz]	0.87 $\pm$ 1.06	2.35 $\pm$ 1.20	0.36 $\pm$ 0.34	2.30 $\pm$ 1.14
Activation damping factor, $\beta$ [–]	0.86 $\pm$ 0.59	1.18 $\pm$ 0.41	0.83 $\pm$ 0.61	1.22 $\pm$ 0.43

Note.—ESWT = extracorporeal shock wave therapy; SD = standard deviation; TS = triceps surae; TA = tibialis anterior. Mean and standard deviation of the estimated condition-dependent model parameters. Condition-dependent parameters were estimated for each trial separately and subsequently averaged over each condition and all subject.

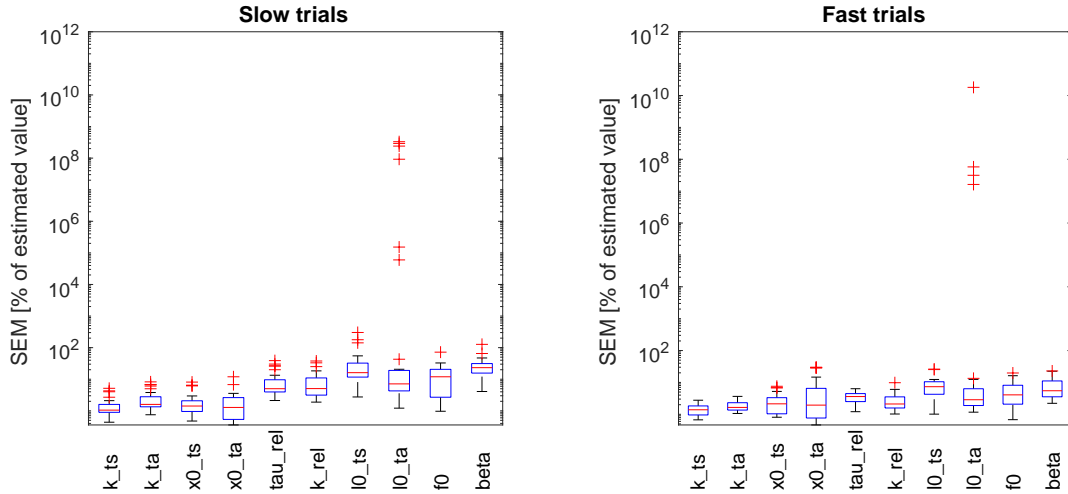


**Figure 5:** Box plot showing the normalized SEM values for the ten condition-dependent parameters. The box plots are shown on a logarithmic range of  $10^2\%$  to  $10^{12}\%$ . Boxes (blue) indicate the first and third quartile, with the median shown as a horizontal bar (red) in between. Minimum and maximum values are indicated by the whiskers (black), with crosses (red) indicating the outliers.

### 3.6. Effect on range of motion

Table 5 shows the measured ROM, including the maximal plantar and dorsiflexion angles ( $\theta_{\max,plantar}$  and  $\theta_{\max,dorsal}$  respectively). A paired-samples t-test showed that there was no statistically significant difference in the mean ROM of the ankle joint after ESWT was applied to patients with chronic muscle hypertonia ( $t(8) = 0.231$ ,  $p = 0.823$ ).

### 3.7. Effect on model parameters

Simple main effect analysis showed that none of the estimated model parameters were significantly affected by a single ESWT session in patients with chronic muscle hypertonia (Table 6).

Simple main effects analysis showed that the stiffness coefficients of the TS  $k_{ts}$  and TA  $k_{ta}$  decreased significantly with movement velocity, ( $F(1,8) = 6.316$ ,

**Table 4:** Condition-independent model parameters

Parameter	Mean $\pm$ SD
<i>Non-neural</i>	
Mass foot and footplate, $m$ [kg]	$1.5 \pm 0.6$
<i>Neural</i>	
EMG weighting factor TA, $g_1$ [1/V]	$(8.8 \pm 9.5) \times 10^7$
EMG weighting factor SOL, $g_2$ [1/V]	$(2.2 \pm 2.9) \times 10^7$
EMG weighting factor GM, $g_3$ [1/V]	$(2.7 \pm 3.0) \times 10^6$
EMG weighting factor GL, $g_4$ [1/V]	$(2.2 \pm 2.1) \times 10^7$

Note.—SD = standard deviation; TA = tibialis anterior; SOL = soleus; GM = gastrocnemius medialis; GL = gastrocnemius lateralis. Mean and standard deviation of the estimated condition-independent model parameters over all subject. Condition-independent parameters were shared between trials of the same subject and therefore were estimated only once for each subject.

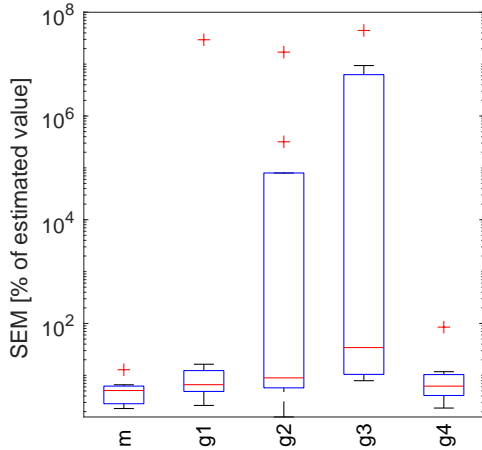


**Figure 6:** Box plot showing the normalized SEM values for the five condition-independent parameters. The box plots are shown on a logarithmic range of 0% to 10<sup>8</sup>%. Boxes (blue) indicate the first and third quartile, with the median shown as a horizontal bar (red) in between. Minimum and maximum values are indicated by the whiskers (black), with crosses (red) indicating the outliers.

$p = 0.036$ ) and ( $F(1, 8) = 9.907$ ,  $p = 0.014$ ) respectively. Muscle slack lengths of the TS  $x_{0,ts}$  and TA  $x_{0,ta}$  decreased significantly with movement velocity, ( $F(1, 8) = 5.806$ ,  $p = 0.043$ ) and ( $F(1, 8) = 8.833$ ,  $p = 0.018$ ) respectively. Tissue relaxation time constant  $\tau_{rel}$  increased significantly with movement velocity

**Table 5:** Measured range of motion

Measure	Pre-ESWT (mean $\pm$ SD)	Post-ESWT (mean $\pm$ SD)
$\theta_{max,plantar}$ [ $^{\circ}$ ]	$-49.4 \pm 7.6$	$-48.9 \pm 9.9$
$\theta_{max,dorsal}$ [ $^{\circ}$ ]	$8.5 \pm 9.5$	$8.6 \pm 10.1$
ROM [ $^{\circ}$ ]	$57.9 \pm 8.6$	$57.5 \pm 10.9$

Note.—ESWT = extracorporeal shock wave therapy; SD = standard deviation; ROM = range of motion. Mean and standard deviation of the measured ROM over all subjects, including the maximal plantar and dorsiflexion angles.

( $F(1, 8) = 6.019$ ,  $p = 0.040$ ). Optimal muscle lengths of the TS  $l_{0,ts}$  and TA  $l_{0,ta}$  decreased significantly with movement velocity, ( $F(1, 8) = 14.196$ ,  $p = 0.005$ ) and ( $F(1, 8) = 5.911$ ,  $p = 0.041$ ) respectively. Activation cut-off frequency  $f_0$  increased significantly with movement velocity ( $F(1, 8) = 26.303$ ,  $p = 0.002$ ). The tissue relaxation factor  $k_{rel}$  and activation damping factor  $\beta$  were not significantly affected by movement velocity.

A two-way repeated measures ANOVA test indicated that there was no statistically significant interaction between the effects of movement velocity and ESWT treatment on the model parameters.

### 3.8. Effect on MAS

A Wilcoxon signed-rank test indicated that MAS grades were significantly lower directly after ESWT treatment in patients with chronic muscle hypertonia ( $Z = -2.121$ ,  $p = 0.034$ ). Indeed, the mean MAS grade was 3.4 pre-ESWT, compared to a mean MAS grade of 2.8 post-ESWT (Table 6).

## 4. Discussion

The overall aim of the current study was to investigate the effect of a single ESWT session on the neural and non-neural contributors to ankle joint resistance in patients with chronic muscle hypertonia ( $MAS > 1$ ), using motorized RaH rotations with different movement velocities and neuromuscular modeling of the ankle joint. The secondary objective was to test the effect of ESWT on the passive ROM and MAS. The validity and agreement of the methods are discussed.

### 4.1. Effect of ESWT

Neither the ROM nor the estimated model parameters were significantly affected by a single ESWT session in patients with chronic muscle hypertonia (see Tables 5 and 6). The absence of an effect is supported by the

**Table 6:** Main outcome measures

Measure	Movement velocity (mean $\pm$ SD)		ESWT treatment (mean $\pm$ SD)	
	Slow	Fast	Pre	Post
<i>Non-neural</i>				
Stiffness coefficient TS, $k_{ts}$ [1/m]	300 $\pm$ 15	265 $\pm$ 12*	284 $\pm$ 10	281 $\pm$ 14
Stiffness coefficient TA, $k_{ta}$ [1/m]	189 $\pm$ 24	141 $\pm$ 21*	170 $\pm$ 21	160 $\pm$ 22
Muscle slack length TS, $x_{0,ts}$ [m]	0.020 $\pm$ 0.001	0.011 $\pm$ 0.001*	0.019 $\pm$ 0.001	0.018 $\pm$ 0.001
Muscle slack length TA, $x_{0,ta}$ [m]	0.062 $\pm$ 0.003	0.045 $\pm$ 0.007*	0.055 $\pm$ 0.004	0.052 $\pm$ 0.006
Tissue relaxation time constant, $\tau_{rel}$ [s]	0.96 $\pm$ 0.21	1.53 $\pm$ 0.34*	1.33 $\pm$ 0.38	1.17 $\pm$ 0.18
Tissue relaxation factor, $k_{rel}$ [-]	0.45 $\pm$ 0.06	0.69 $\pm$ 0.17	0.54 $\pm$ 0.11	0.60 $\pm$ 0.13
<i>Neural</i>				
Optimal muscle length TS, $l_{0,ts}$ [m]	0.082 $\pm$ 0.003	0.053 $\pm$ 0.005*	0.065 $\pm$ 0.001	0.070 $\pm$ 0.004
Optimal muscle length TA, $l_{0,ta}$ [m]	0.070 $\pm$ 0.005	0.052 $\pm$ 0.007*	0.067 $\pm$ 0.007	0.055 $\pm$ 0.004
Activation cut-off frequency, $f_0$ [Hz]	0.62 $\pm$ 0.15	2.33 $\pm$ 0.35*	1.61 $\pm$ 0.26	1.33 $\pm$ 0.19
Activation damping factor, $\beta$ [-]	0.84 $\pm$ 0.14	1.20 $\pm$ 0.11	1.02 $\pm$ 0.11	1.02 $\pm$ 0.10
<i>Clinical</i>				
MAS [-]	-	-	3.4 $\pm$ 0.7	2.8 $\pm$ 0.7*

Note.—ESWT = extracorporeal shock wave therapy; SD = standard deviation; TS = triceps surae; TA = tibialis anterior; MAS = Modified Ashworth Scale. Values shown are the combined results of Table 3 for both test factors: *movement velocity* and *ESWT treatment*. For example, values shown under the first column (*slow movement velocity*) are the combined results of slow trials for both pre- and post-ESWT treatment. Similarly, values shown under the third column (*pre-ESWT treatment*) are the combined results of both the slow and fast trials, both pre-ESWT. The same applies to the other columns.

\* Statistically significant,  $p < 0.05$ .

measured torque data as shown in Appendix B. Here, no strong visual difference is observed in the measured torque profiles between pre-treatment (cyan/blue traces) and post-treatment (purple/pink traces), for each movement velocity (see Figures C.8 to C.16). In other words, the resistance as measured by the robotic manipulator was similar between RaH movements before and after ESWT treatment, with the same movement velocity. Since no effect of ESWT on the model parameters and ROM was found, the effect of ESWT on the neural and non-neural contributors of joint resistance in patients with chronic muscle hypertonia remains unknown.

In contrast to the results on the model parameters and ROM, the MAS was significantly lower after ESWT treatment, which is in line with previous studies [8–18]. One of these studies also found an effect of ESWT on the MAS, whereas no change was observed in the measured ROM [13].

The disagreement between the results of the estimated model parameters and ROM, and the MAS raises some questions about the validity of the Ashworth test to assess muscle hypertonia. As was discussed previously, the Ashworth test is a subjective test which grades the severity of muscle hypertonia on an ordinal scale. The result on the MAS should therefore be taken with care.

#### 4.2. Effect of movement velocity

Movement velocity showed a significant change in model parameters of both the intrinsic (stiffness coefficients  $k_{ts}$  and  $k_{ta}$ , muscle slack lengths  $x_{0,ts}$  and  $x_{0,ta}$ , and tissue relaxation time constant  $\tau_{rel}$ ) and neural part (optimal muscle lengths  $l_{0,ts}$  and  $l_{0,ta}$ , and activation cut-off frequency  $f_0$ ) of the system. Since spasticity is known to be velocity-dependent, a difference in the total measured torque between the slow and fast trials is to be expected. Indeed, as shown by the measured torque data in Appendix B, the resistance reaches higher peaks during the first ramp phase of the fast trials (see Figures C.8 to C.16). This increase in resistance is often due to increased reflex activity (as shown in the EMG data), which is present during the faster movements.

#### 4.3. Model validity

The high VAF values for the optimized model fits indicate that the observed ankle torque could be well described by the neuromuscular model, which is in line with previous versions of the model [22–25]. Model fits for the slow trials (mean VAF 99.9%) were better than for the fast trials (mean VAF 99.5%), although both were generally very high.

The full model consists of 15 optimizable parameters. Sensitivity and the absence of redundancy within

the model parameters was tested using the standard error of the mean (SEM). The sensitivity was high (low SEM values) for most parameters, except for the EMG weighting factors of the soleus ( $g_2$ ) and gastrocnemius medialis ( $g_3$ ). For these two parameters, extremely large SEM values were found, which indicates that they had little to no contribution to the total modeled output torque, and therefore may be redundant. This result is to be expected since the torque generated by the TS is dependent on its neural input, which in turn is a linear combination of the weighting factors and their corresponding muscle EMG (SOL, GM, GL). Since similar EMG behavior is observed during contraction of the TS muscles (simultaneous contraction), the optimization process is free to select which muscles contributed to the model torque, and to what extent. As a result, only one of these three weighting factors ( $g_2 - g_4$ ) may be sufficient to describe the active torque from the TS.

Further observations of the SEM values showed that the model parameters of the muscle visco-elastic components (stiffness coefficients  $k_{ts}$  and  $k_{ta}$ , muscle slack lengths  $x_{0,ts}$  and  $x_{0,ta}$ , and tissue relaxation time constant  $\tau_{rel}$  and factor  $k_{rel}$ ) were estimated reliably for both the slow (median SEM < 5 %) and fast (median SEM < 4 %) trials. Low SEM values for these parameters indicate that these parameters were estimated accurately, and have substantial contribution to the total modeled output torque. Model parameters of the neural components (optimal muscle lengths  $l_{0,ts}$  and  $l_{0,ta}$ , and activation cut-off frequency  $f_0$  and damping factor  $\beta$ ) were estimated more reliable for the fast trials (median SEM < 8 %) than for the slow trials (median SEM < 24 %). Relatively high SEM values for these parameters during the slow trials means that they only had a small contribution to the total modeled output torque for this condition. This result is to be expected since the active muscle torques are calculated from their corresponding neural input. If little to no muscle activation (EMG) is observed, contributions of the active muscle torques to the total modeled output torque is minimal and may result in badly scaled parameters.

RaH trials were performed twice for each condition to test for repeatability of the estimation procedure. Inter-trial repeatability was examined by using the intraclass correlation coefficient (ICC). Repeatability of the estimation process between two repeated trials was good (median ICC: 0.837), except for the optimal muscle length of the TA (ICC: 0.357). However, this ICC is computed over both the slow and fast trials simultaneously. When separating the slow from the fast trials, the ICC for the optimal muscle length  $l_{0,ta}$  is  $-0.083$  for the slow, and  $0.588$  for the fast trials. These values are

still not very good, but at least give a better insight as to why the combined ICC was so low. The very low ICC for the slow condition may be the result of badly scaled parameters, as was shown by the SEM.

Due to absence of sufficient muscle activity, parameters of the neural components could not be estimated accurately and may differ in value between different RaH trials. This was especially the case in the slow trials. In these situations, the total neuromuscular model becomes over-parameterized, resulting in redundancy of the parameters. When parameters become redundant, they may show large variances in their estimated values. The increase in variance of the parameter value may therefore negatively impact the results (as was shown by the repeatability), and decrease the sensitivity of possible effects (in case they would be present).

#### 4.4. RaH movement versus Ashworth test

It is important to note that the results from the neuromuscular modeling cannot be directly compared to the results from the Ashworth test. As per definition, the Ashworth test measures the resistance to passive stretch as felt by the examiner during a passive, one second joint rotation over its full range of motion. This results in a few differences between the Ashworth test and the instrumented RaH rotation as applied in the current study. For one, the instrumented RaH movement were applied with a fixed constant velocity, whereas manually imposed rotations may result in a bell-shaped velocity profile. Furthermore, the Ashworth test measures the resistance over the full range of motion during a one second joint rotation. Depending on the ROM of the corresponding joint in question, the velocity with which the movement takes place may vary. For example, in the current study the average measured ROM was roughly  $60^\circ$ . Assuming that the Ashworth test was performed in 1 s, the movement velocity with which the clinical test was performed would then be  $60^\circ/s$  on average. This is about half of the movement velocity of the instrumented fast trial. Therefore, resistances resulting from stretch reflexes may be different between the instrumented RaH movement, and the Ashworth test.

#### 4.5. Treatment protocol settings

The treatment protocol in the current study was based of the protocol from Vidal et al. (2011) [17]. However, different studies treated different muscles with different settings (i.e. energy level, number of pulses, frequency) of their ESWT treatment protocol to investigate the efficacy of ESWT on muscle hypertonia. For example, Manganotti et al. (2015) found a much larger decrease

in MAS for the finger flexors, compared to the wrist flexors [8]. The combination of muscle size and ESWT settings may play a large role in the outcome of the results.

#### 4.6. Limitations

##### 4.6.1. Simplified joint physiology

The neuromuscular model used in this study is a simplification of the real ankle joint physiology. Ankle joint rotations were assumed to be uniaxial, described by  $\theta(t)$  in the model. However, in reality, the foot is a multi-joint structure which allows for multiple movements such as dorsi- and plantar flexion, as well as inversion and eversion of the foot [30]. Movements of the foot in undesirable directions were minimized by strapping the foot to a footplate using Velcro straps and manually aligning the axis of rotation of the ankle joint with that of the Achilles motor. Limited accuracy in manually aligning the two axes may not always result in a perfectly aligned situation. As a result, rotation of the ankle may not always be a perfect uniaxial rotation, but rather rotate around a moving axis.

Muscle lengths  $x_m(\theta)$  and tendon moment arms  $r_m(\theta)$  were assumed to scale linearly with joint angle. However, for this study, a wide variety of subjects were recruited. Patients of different ages and with different time after the onset of their accident may vary in size and deformation in the lower extremities. Therefore, linearization of the muscle lengths and tendon moment arms may not be an accurate representation for all subjects.

Muscle connective tissue of the dorsi- and plantar flexors were modeled as lumped components. The triceps surae is a muscle group consisting of three muscles (the soleus and both gastrocnemii) but was modeled as a single muscle. Model parameters representing the physiology of the muscle connective tissue are therefore only simplifications of the real muscle physiology. Furthermore, muscle activation dynamics (slow and fast fiber types) and muscle structure (pennation angle, muscle fibers, and tendon) were not accurately represented. For example, pennation angles were defined to be zero and as a result, muscle and fiber length were assumed to be equal [23]. Furthermore, tendons were assumed to be infinitely stiff. It was shown by a previous MSc thesis that the inclusion of tendon dynamics did not improve the model optimization process, and were therefore left out of the model [31].

Although the model is a simplification of the joint physiology, it appeared to be able to discriminate in neural and non-neural contributors to muscle hypertonia between patients with stroke or CP, and healthy controls [22–25].

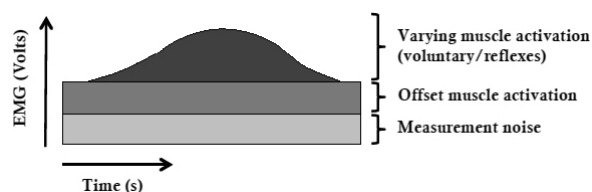


**Figure 7:** Composition of the measured EMG signals. Total EMG is assumed to consist of a varying part (representing active, or reflexive muscle contraction), and an offset part. The offset is assumed to consist of both background muscle activation as well as measurement noise. Image from [32].

##### 4.6.2. EMG offset

To investigate the effect of increased reflex activity on the model parameters, the offset EMG activity was eliminated from the total EMG. This step was done in order to eliminate any background measurement noise that may be present in the EMG data. However, this offset EMG not only consists of background measurement noise, it also consists of background muscle activity (Figure 7). Since measurement noise and background muscle activity are difficult to distinguish from each other, the total EMG offset was removed from each measured EMG signal. However, in doing so, an important part of the system (that is background muscle activity) contributing to the total dynamical behavior of the joint is not captured by the model. As a result, the neural torque contributing to the total joint torque may be underestimated. For future research, a method that can distinguish between measurement noise and background (offset) muscle EMG is desired in order to capture the full dynamics of muscle contraction.

##### 4.6.3. Patient diversity

The sample size of the current study consists of a total of nine patients with chronic muscle hypertonia. This number of subjects may not be sufficient enough to represent the total population well. However, subject recruitment in the given amount of time deemed difficult. Many patients were already being treated with botulinum toxin, which automatically excluded the majority of the available candidates. Consequently, patients with different movement disorders (e.g. stroke, traumatic brain injury, and cerebral palsy) were recruited. Even though each subject was diagnosed with chronic muscle hypertonia, depending on the origin and location of the lesion, pathophysiology of the muscle hypertonia may differ between subjects. Furthermore, age and time after onset of the accident may play a large role in the pathophysiology of each patient as well [33]. Therefore, when studying a population like this with only a small

number and wide variety of participants, a case study (or individual analysis of the results) may be preferred.

#### 4.7. Future research

For future research, model validity and parameter accuracy can be improved by using richer data for the parameter optimization procedure. For example, model parameters that describe the neural components of the joint resistance can only be estimated accurately during trials in which there is enough muscle activity. A possible solution to improve the parameter estimation procedure, is to estimate the model parameters in one estimation process over a combined slow and fast trial, or over RaH trials that have multiple movement velocities incorporated in them (as was done by de Gooijer-van de Groep et al. (2016)). By applying this method, intrinsic components could be estimated reliable due to the slow movement, whereas neural components could be estimated reliable due to the fast movement, both in one procedure. Furthermore, incorporating different movement velocities into one estimation process gives richer data for the model to describe the velocity-dependent components such as the muscle force-velocity characteristics, and ensures that enough muscle EMG is present.

The model parameters of the neuromuscular model are defined on the linear muscle level. For future research, it may be interesting to investigate the relation between the model parameters at muscle level, and the resulting passive and reflexive stiffness at joint level. For example, the passive stiffness profile (as described by the interaction between the muscle stiffness coefficient  $k_m$  and slack length  $x_{0,m}$ ) as result of the joint angle would be interesting to investigate. By investigating the resistance of the different system components at joint level, the effect of treatment modalities such as ESWT on muscle hypertonia may be better understood.

## 5. Conclusion

Neuromuscular modeling in combination with motorized ramp-and-hold movements enabled us to estimate model parameters representing the neural and non-neural contributors of the total ankle joint, in patients with chronic muscle hypertonia. The effect of extracorporeal shock wave therapy was investigated. Conclusions are summarized as follows:

- The method yielded estimated model parameters which were estimated with average to good reliability and resulted in good model fits.
- No effect of a ESWT was observed on the estimated model parameters and the passive ROM.

- The MAS was significantly lower after ESWT, which raises questions about the validity of the Ashworth test.
- No conclusion can be drawn on the effect of ESWT on the neural and non-neural contributors to joint resistance in patients with chronic muscle hypertonia.
- The model parameter estimation procedure can be improved by using richer data, e.g. trials which include both slow and fast movement velocities.

## A. Neuromuscular Model

The observed ankle torque from RaH rotations can be described by a nonlinear neuromuscular model that can discriminate between neural and non-neural components by optimizing 15 physiological interpretable parameters. The model was originally developed by de Vlught et al. (2010) [22], and has had a few alterations over the years [23–25].

The total ankle joint resistance is described by:

$$T_{\text{mod}}(t) = I\ddot{\theta}(t) + T_{\text{grav}}(\theta) + T_{\text{ts}}(t) - T_{\text{ta}}(t) \quad (\text{A.1})$$

where  $t$  represents the independent time variable in [s],  $T_{\text{mod}}(t)$  the modeled ankle reaction torque in [Nm],  $\theta(t)$  the measured ankle joint angle in [rad],  $\ddot{\theta}(t)$  the ankle joint angular acceleration in [ $\text{rad}/\text{s}^2$ ],  $I$  the inertia of the ankle plus footplate in [ $\text{kg m}^2$ ],  $T_{\text{grav}}(\theta)$  the torque due to gravitation in [Nm],  $T_{\text{ts}}(t)$  the torque generated by the triceps surae (TS: SOL, GM, GL) in [Nm], and  $T_{\text{ta}}(t)$  the torque generated by the tibialis anterior (TA) in [Nm].

The inertia of the ankle plus footplate is modeled as a point mass  $m$  in [kg] at a distance  $l_a$  (fixed at 0.1 m) from the axis of rotation:

$$I = ml_a^2 \quad (\text{A.2})$$

Torque due to gravitation is described by:

$$T_{\text{grav}}(\theta) = mgl_a \cos(\theta(t) + \theta_{\text{gnd}}) \quad (\text{A.3})$$

where  $\theta_{\text{gnd}}$  represents the angle of the foot and footplate with respect to the ground (horizontal) in [rad], and  $g$  the gravitational acceleration of  $9.8 \text{ m}/\text{s}^2$ .

Muscle torques for the plantar flexion and dorsiflexion muscles are described by:

$$T_m(t) = (F_{\text{elas},m}(t) + F_{\text{act},m}(t))r_m(\theta) \quad (\text{A.4})$$

where  $m$  represents the muscle group (TS and TA),  $F_{\text{elas},m}(t)$  the elastic force of the parallel connective

tissue in [N],  $F_{\text{act,m}}(t)$  the active muscle force generated from muscle contraction, according to the Hill-type muscle model in [N], and  $r_m(\theta)$  the angle dependent moment arm of the muscle tendon in [m].

Moment arms for the TS and TA are assumed to scale linearly with joint angle, as derived from [34, 35], and can be described by:

$$r_{\text{ts}}(\theta) = 0.0480 - 0.0104\theta(t) \quad (\text{A.5})$$

$$r_{\text{ta}}(\theta) = 0.0393 + 0.0171\theta(t) \quad (\text{A.6})$$

where  $r_{\text{ts}}(\theta)$  represents the moment arm of the TS, and  $r_{\text{ta}}(\theta)$  the moment arm of the TA.

The elastic force components for the plantar flexion and dorsiflexion muscles are described by:

$$F_{\text{elas,m}}(t) = e^{k_m(x_m(t)-x_{0,m})} \quad (\text{A.7})$$

where  $k_m$  is the estimated stiffness coefficient of the muscle in [1/m],  $x_m(t)$  the muscle length (linear displacement) in [m], and  $x_{0,m}$  the estimated slack length of the connective tissue in [m]. The shape of the elastic force curve is determined by the stiffness coefficient  $k_m$  and the muscle slack length  $x_{0,m}$ . The latter being defined as the length for which the elastic muscle force starts to increase, when the muscle is stretched beyond this length.

Muscle lengths of the TS and TA are dependent on their initial muscle length at a joint angle of 0 rad (taken from [34, 35]), and their corresponding moment arms, and can be described by:

$$x_{\text{ts}}(\theta) = 0.118 - 1.67r_{\text{ts}}(\theta) \quad (\text{A.8})$$

$$x_{\text{ta}}(\theta) = 0.136 - 1.56r_{\text{ta}}(\theta) \quad (\text{A.9})$$

where  $x_{\text{ts}}(\theta)$  represents the muscle length of the TS, and  $x_{\text{ta}}(\theta)$  the muscle length of the TA. Take note that the muscle length of the TS scales negatively with its moment arm, which in turn scales negatively with joint angle. As a result, the muscle length of the TS scales positively with joint angle. Similarly, the muscle length of the TA scales negatively with joint angle. Positive values for joint angle  $\theta(t)$  were defined as dorsiflexion, and thus movement in dorsiflexion direction causes lengthening of the TS, and shortening of the TA.

Muscle connective tissue under tension exhibits relaxation or force decrease [26–28], which is modeled by a first order filter, according to:

$$F_{\text{elas,m}}(s) = \frac{\tau_{\text{rel}}s + 1}{\tau_{\text{rel}}s + 1 + k_{\text{rel}}} F_{\text{elas,m}}(s) \quad (\text{A.10})$$

where  $\tau_{\text{rel}}$  is the estimated tissue relaxation time constant in [s],  $k_{\text{rel}}$  the estimated tissue relaxation factor,

and  $s$  the Laplace operator denoting the first time derivative. Furthermore, elastic forces in negative direction were set to zero, as connective tissue can only exert pulling forces, according to:

$$F_{\text{elas,m}}(t) = \begin{cases} F_{\text{elas,m}}(t) & \text{for } F_{\text{elas,m}}(t) \geq 0 \\ 0 & \text{for } F_{\text{elas,m}}(t) < 0 \end{cases} \quad (\text{A.11})$$

The active muscle force components for the plantar flexion and dorsiflexion muscles are estimated from their corresponding neural activity, described as:

$$u_{\text{ta}}(t) = g_1 EMG_{\text{TA}}(t) \quad (\text{A.12})$$

$$u_{\text{ts}}(t) = g_2 EMG_{\text{SOL}}(t) + g_3 EMG_{\text{GM}}(t) + g_4 EMG_{\text{GM}}(t) \quad (\text{A.13})$$

where  $u_{\text{ta}}(t)$  and  $u_{\text{ts}}(t)$  represent the neural activity for the TA and TS respectively,  $EMG_m(t)$  the measured EMG signals of the TA, SOL, GM and GL respectively, and  $g_1 - g_4$  the weighting factors of their corresponding muscles.

The neural activity is then filtered by a linear second order filter describing the muscle activation process to produce the active state of the muscle [22]. The filter is described by:

$$\alpha_m(s) = \frac{\omega_0^2}{s^2 + 2\beta\omega_0s + \omega_0^2} u_m(s) \quad (\text{A.14})$$

where  $\alpha_m(s)$  is the active state of the muscle,  $\omega_0 = 2\pi f_0$  the estimated cut-off frequency,  $\beta$  the estimated activation damping factor, and  $s$  the Laplace operator denoting the first time derivative.

A Hill-type muscle model was used to compute the active muscle force using the active muscle state, force-length and force-velocity characteristics of the muscle, according to:

$$F_{\text{act,m}}(t) = f_l(x_m)f_v(\dot{x}_m)\alpha_m \quad (\text{A.15})$$

where  $f_l(x_m)$  represents the force-length relationship, and  $f_v(\dot{x}_m)$  the force-velocity relationship of the corresponding muscle.

The muscle force-length relationship is described by:

$$f_l(x_m) = e^{-\frac{(x_m - l_{0,m})^2}{w_{\text{fl,m}}}} \quad (\text{A.16})$$

where  $l_{0,m}$  is the estimated optimal muscle length of the TS and TA in [m], and  $w_{\text{fl,m}}$  a shaping factor defined as:

$$w_{\text{fl,m}} = c_f l_{0,m}^2 \quad (\text{A.17})$$

where  $c_f$  represents the shape parameter of the force-length relationship, which is set to 0.5, from Slood et al. (2015) [25].

The muscle force-velocity characteristics were taken from [36] and are described by:

$$f_v(\dot{x}_m) = \begin{cases} 1 - \frac{(1+m_{vsh}m_{vshl})(f_{ecc}-1)\dot{x}_m}{m_{vsh}m_{vshl}v_{max,m}+\dot{x}_m} & \text{for } \dot{x}_m \geq 0 \\ \frac{\dot{x}_m+v_{max,m}}{m_{vsh}-v_{max,m}} & \text{for } \dot{x}_m < 0 \end{cases} \quad (\text{A.18})$$

where  $m_{vsh}$  and  $m_{vshl}$  are shaping factors with values 0.25 and 0.5 respectively;  $v_{max,m}$  is the maximum shortening velocity which was set to 8 times the optimal muscle length;  $f_{ecc}$  is the the maximum eccentric force which was set to 1.5 times the isometric force and the isometric force was normalized to 1 because scaling of force was full determined by the EMG weighting factors  $g_1 - g_4$  [22].

## B. Measured data

See Figures C.8 to C.16.

## C. Model fits

See Figures C.17 to C.25.

## References

- [1] V. Dietz, T. Sinkjaer, Spastic movement disorder: impaired reflex function and altered muscle mechanics, *The Lancet Neurology* 6 (8) (2007) 725–733. doi:10.1016/S1474-4422(07)70193-X.
- [2] J. W. Lance, Symposium synopsis, in: R. G. Feldman, R. R. Young, W. P. Koella (Eds.), *Spasticity: disordered motor control*, Year Book Medical Publishing, Chicago, 1980, pp. 485–494.
- [3] G. Sheean, The pathophysiology of spasticity, *European Journal of Neurology* 9 (s1) (2002) 3–9. doi:10.1046/j.1468-1331.2002.0090s1003.x.
- [4] M. E. Gormley, C. F. O'Brien, S. A. Yablon, A clinical overview of treatment decisions in the management of spasticity, *Muscle & Nerve* 20 (S6) (1997) 14–20. doi:10.1002/(sici)1097-4598(1997)6+<14::aid-mus3>3.3.co;2-s.
- [5] V. L. Stevenson, Rehabilitation in practice: Spasticity management, *Clinical Rehabilitation* 24 (4) (2010) 293–304. doi:10.1177/0269215509353254.
- [6] C.-J. Wang, Extracorporeal shockwave therapy in musculoskeletal disorders, *Journal of Orthopaedic Surgery and Research* 7 (1) (2012) 11. doi:10.1186/1749-799X-7-11.
- [7] J. A. Ogden, A. Tóth-Kischkat, R. Schultheiss, Principles of shock wave therapy, *Clinical Orthopaedics and Related Research* 387 (2001) 8–17. doi:10.1097/00003086-200106000-00003.
- [8] P. Manganotti, E. Amelio, Long-term effect of shock wave therapy on upper limb hypertonia in patients affected by stroke, *Stroke* 36 (9) (2005) 1967–1971. doi:10.1161/01.STR.0000177880.06663.5c.
- [9] H. Bae, J. M. Lee, K. H. Lee, The effects of extracorporeal shock wave therapy on spasticity in chronic stroke patients., *Journal of Korean Academy of Rehabilitation Medicine* 34 (6) (2010) 663–669.
- [10] M. K. Sohn, K. H. Cho, Y.-J. Kim, S. L. Hwang, Spasticity and electrophysiologic changes after extracorporeal shock wave therapy on gastrocnemius, *Annals of Rehabilitation Medicine* 35 (5) (2011) 599. doi:10.5535/arm.2011.35.5.599.
- [11] F. Troncati, M. Paci, T. Myftari, B. Lombardi, Extracorporeal shock wave therapy reduces upper limb spasticity and improves motricity in patients with chronic hemiplegia: A case series, *NeuroRehabilitation* 33 (3) (2013) 399–405. doi:10.3233/NRE-130970.
- [12] Y. W. Kim, J. C. Shin, J. G. Yoon, S. C. Lee, Usefulness of radial extracorporeal shock wave therapy for the spasticity of the subscapularis in patients with stroke: A pilot study, *Chinese medicine journal* 126 (24) (2013) 4638–4643. doi:10.3760/cma.j.issn.0366-6999.20131129.
- [13] S. W. Moon, J. H. Kim, M. J. Jung, S. Son, J. H. Lee, H. Shin, E. S. Lee, C. H. Yoon, M.-K. Oh, The effect of extracorporeal shock wave therapy on lower limb spasticity in subacute stroke patients, *Annals of Rehabilitation Medicine* 37 (4) (2013) 461–470. doi:10.5535/arm.2013.37.4.461.
- [14] S. S. Daliri, B. Forogh, S. Z. E. Razavi, T. Ahadi, F. Madjlesi, N. N. Ansari, A single blind, clinical trial to investigate the effects of a single session extracorporeal shock wave therapy on wrist flexor spasticity after stroke, *Neurorehabilitation* 36 (1) (2015) 67–72. doi:10.3233/NRE-141193.
- [15] K. Z. Fouda, M. A. Sharaf, Efficacy of radial shock wave therapy on spasticity in stroke patients, *International Journal of Health and Rehabilitation Sciences (IJHRS)* 4 (1) (2015) 19. doi:10.5455/ijhrs.000000072.
- [16] E. Amelio, P. Manganotti, Effect of shock wave stimulation on hypertonic plantar flexor muscles in patients with cerebral palsy: A placebo-controlled study, *Journal of Rehabilitation Medicine* 42 (4) (2010) 339–343. doi:10.2340/16501977-0522.
- [17] X. Vidal, A. Morral, L. Costa, M. Tur, Radial extracorporeal shock wave therapy (reswt) in the treatment of spasticity in cerebral palsy: A randomized, placebo-controlled clinical trial, *Neurorehabilitation* 29 (4) (2011) 413–419. doi:10.3233/NRE-2011-0720.
- [18] M. I. Gonkova, E. M. Ilieva, G. Ferriero, I. Chavdarov, Effect of radial shock wave therapy on muscle spasticity in children with cerebral palsy, *International Journal of Rehabilitation Research* 36 (3) (2013) 284–290. doi:10.1097/MRR.0b013e328360e51d.
- [19] B. Ashworth, Preliminary trial of carisoprodol in multiple sclerosis, *Practitioner* 192 (1964) 540–542.
- [20] R. W. Bohannon, M. B. Smith, Interrater reliability of a modified ashworth scale of muscle spasticity, *Physical Therapy* 67 (2) (1987) 206–207.
- [21] A. Santamato, M. F. Micello, F. Panza, F. Fortunato, G. Logroscino, A. Picelli, P. Manganotti, N. Smania, P. Fiore, M. Ranieri, Extracorporeal shock wave therapy for the treatment of post-stroke plantar-flexor muscles spasticity: A prospective open-label study, *Topics in Stroke Rehabilitation* 21 (sup1) (2014) S17–S24. doi:10.1310/tsr21S1-S17.
- [22] E. de Vlugt, J. H. de Groot, K. E. Schenkeveld, J. H. Arendzen, F. C. van der Helm, C. G. Meskers, The relation between neuromechanical parameters and ashworth score in stroke patients, *Journal of NeuroEngineering and Rehabilitation* 7 (1) (2010) 35. doi:10.1186/1743-0003-7-35.
- [23] K. L. de Gooijer-van de Groep, E. de Vlugt, H. J. van der Krogt, Á. Helgadottir, J. H. Arendzen, C. G. M. Meskers, J. H. de Groot, Estimation of tissue stiffness, reflex activity, optimal

- muscle length and slack length in stroke patients using an electromyography driven antagonistic wrist model, *Clinical Biomechanics* 35 (2016) 93–101. doi:10.1016/j.clinbiomech.2016.03.012.
- [24] K. L. de Gooijer-van de Groep, E. de Vlugt, J. H. de Groot, H. C. M. van der Heijden-Maessen, D. H. M. Wielheesen, R. M. S. van Wijlen-Hempel, J. H. Arendzen, C. G. M. Meskers, Differentiation between non-neural and neural contributors to ankle joint stiffness in cerebral palsy, *Journal of NeuroEngineering and Rehabilitation* 10 (81). doi:10.1186/1743-0003-10-81.
- [25] L. H. Sloot, M. M. van der Krogt, K. L. de Gooijer-van de Groep, S. van Eesbeek, J. H. de Groot, A. I. Buizer, C. G. M. Meskers, J. G. Becher, E. de Vlugt, J. Harlaar, The validity and reliability of modelled neural and tissue properties of the ankle muscles in children with cerebral palsy, *Gait & Posture* 42 (1) (2015) 7–15. doi:10.1016/j.gaitpost.2015.04.006.
- [26] S. P. Magnusson, E. B. Simonsen, P. Dyhre-Poulsen, P. Aagaard, T. Mohr, M. Kjaer, Viscoelastic stress relaxation during static stretch in human skeletal muscle in the absence of emg activity, *Scandinavian Journal of Medicine & Science in Sports* 6 (6) (1996) 323–328. doi:10.1111/j.1600-0838.1996.tb00101.x.
- [27] P. J. McNair, E. W. Dombroski, D. J. Hewson, S. N. Stanley, Stretching at the ankle joint: viscoelastic responses to holds and continuous passive motion, *Wilderness & Environmental Medicine* 12 (3) (2001) 215–216. doi:10.1097/00005768-200103000-00003.
- [28] E. Bressel, P. J. McNair, The effect of prolonged static and cyclic stretching on ankle joint stiffness, torque relaxation, and gait in people with stroke, *Physical Therapy* 82 (9) (2002) 880–887. doi:10.1093/ptj/82.9.880.
- [29] L. Ljung, *System Identification - Theory for the User*, 2nd Edition, Prentice Hall, Upper Saddle River, New Jersey, 1999.
- [30] E. N. Marieb, K. Hoehn, *Human Anatomy & Physiology*, 9th Edition, Pearson, 2012.
- [31] K. D. van de Poll, Estimating ankle muscle parameters. developing a tendon dynamics included neuromechanical muscle model and expanding the measurement protocols to improve ankle muscle parameter estimation accuracy, *mathesis*, Delft University of Technology (Jan. 2016).
- [32] Á. Helgadóttir, Identification of muscle activation at rest, *mathesis*, Delft University of Technology (Jun. 2013).
- [33] M. M. Mirbagheri, C. Tsao, K. Settle, T. Lilaonitkul, W. Z. Rymer, Time course of changes in neuromuscular properties following stroke, in: 2008 30th Annual International Conference of the IEEE Engineering in Medicine and Biology Society, IEEE, 2008, pp. 5097–5100. doi:10.1109/IEMBS.2008.4650360.
- [34] C. N. Maganaris, V. Baltzopoulos, A. J. Sargeant, In vivo measurements of the triceps surae complex architecture in man: implications for muscle function, *The Journal of Physiology* 512 (2) (1998) 603–614. doi:10.1111/j.1469-7793.1998.603be.x.
- [35] C. N. Maganaris, V. Baltzopoulos, Predictability of in vivo changes in pennation angle of human tibialis anterior muscle from rest to maximum isometric dorsiflexion, *European Journal of Applied Physiology and Occupational Physiology* 79 (3) (1999) 294–297. doi:10.1007/s004210050510.
- [36] D. G. Thelen, Adjustment of muscle mechanics model parameters to simulate dynamic contractions in older adults, *Journal of Biomechanical Engineering* 125 (1) (2003) 70–77. doi:10.1115/1.1531112.

Subject 1

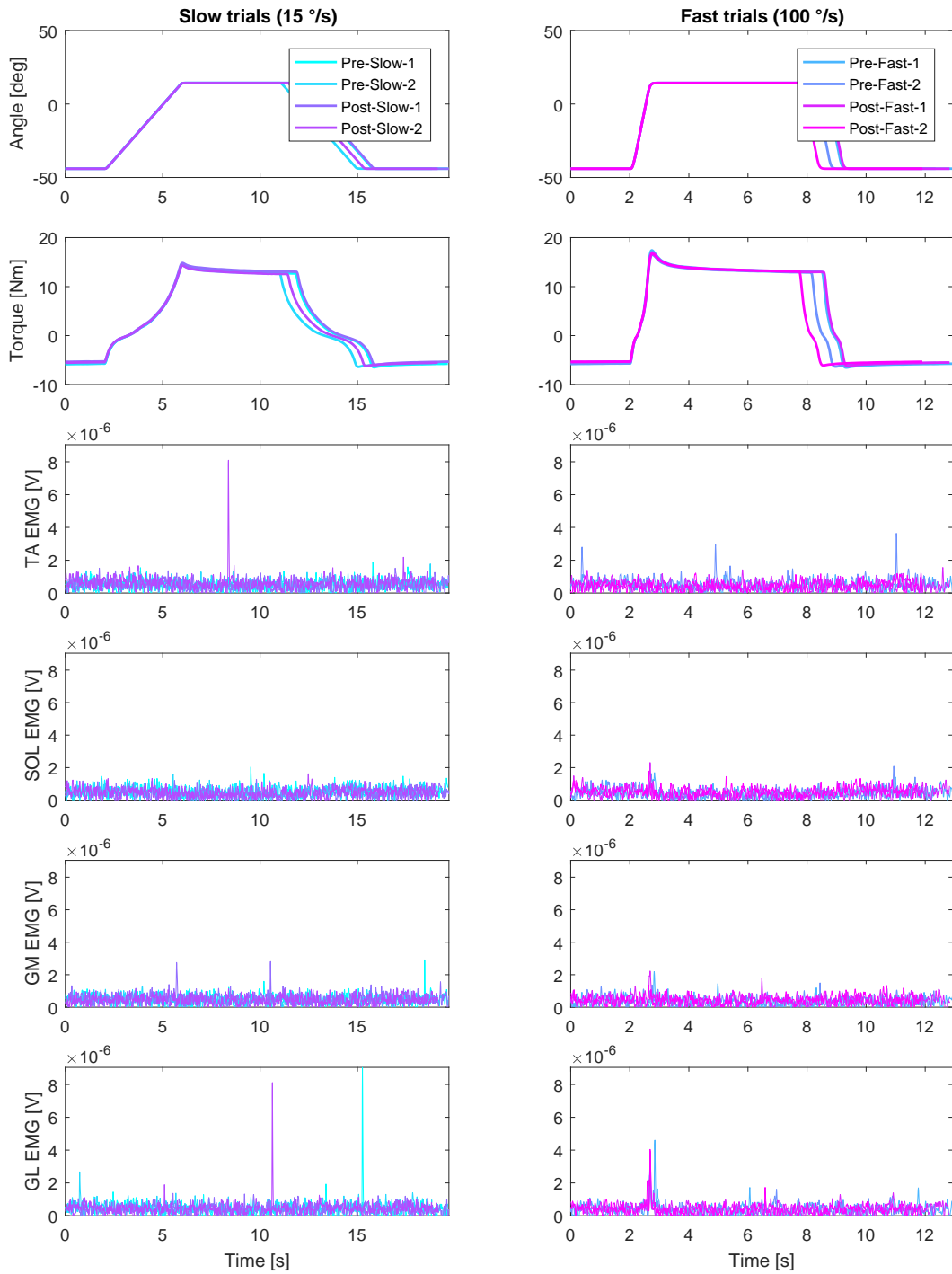


**Figure C.8:** Measured data for Subject 1. From top to bottom: imposed RaH movement profiles, measured joint torque, and muscle EMG from the TA, SOL, GM and GL respectively. Left column: slow trials. Right column: fast trials.

Subject 2

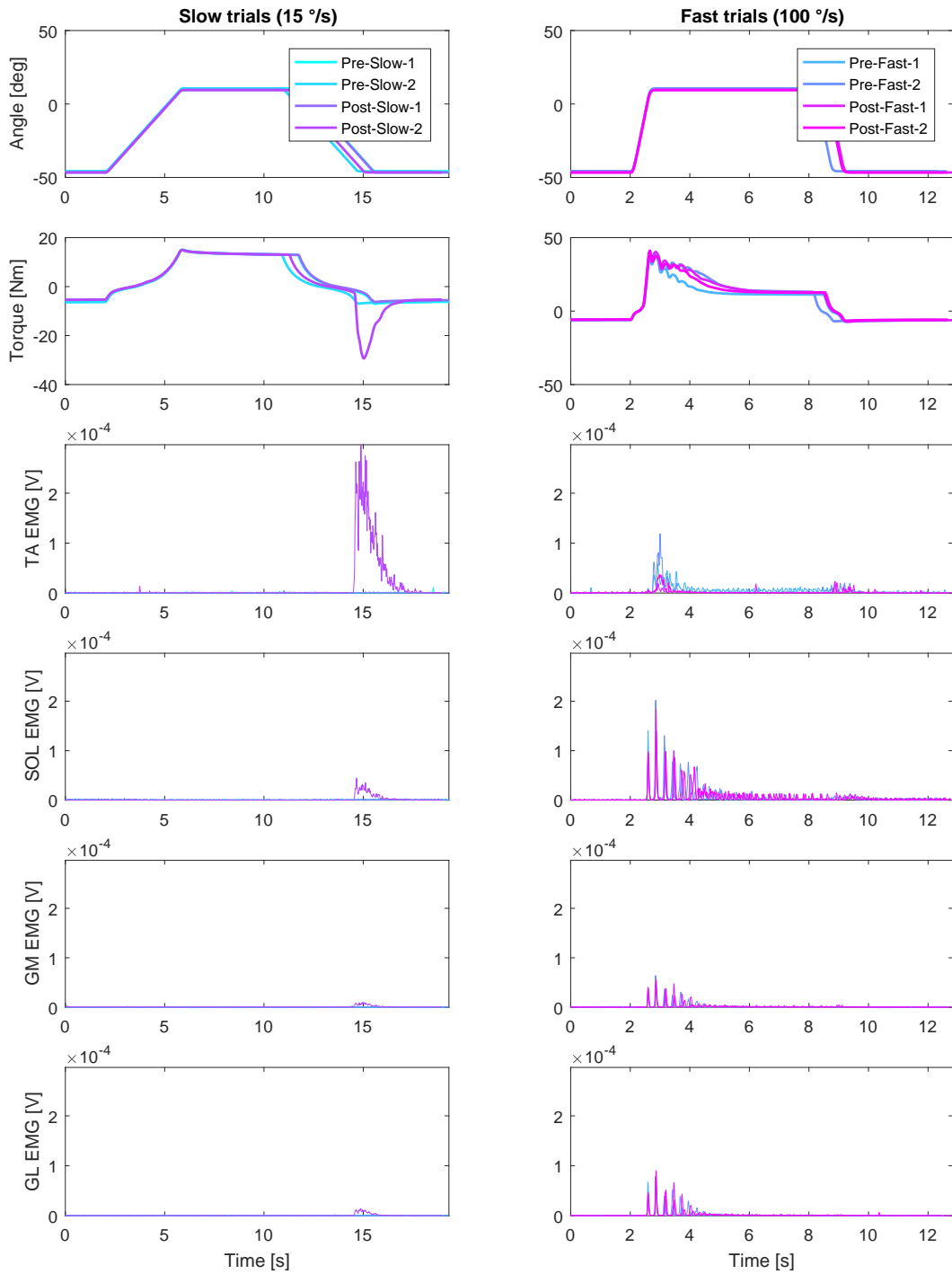


**Figure C.9:** Measured data for Subject 2. From top to bottom: imposed RaH movement profiles, measured joint torque, and muscle EMG from the TA, SOL, GM and GL respectively. Left column: slow trials. Right column: fast trials.

Subject 3

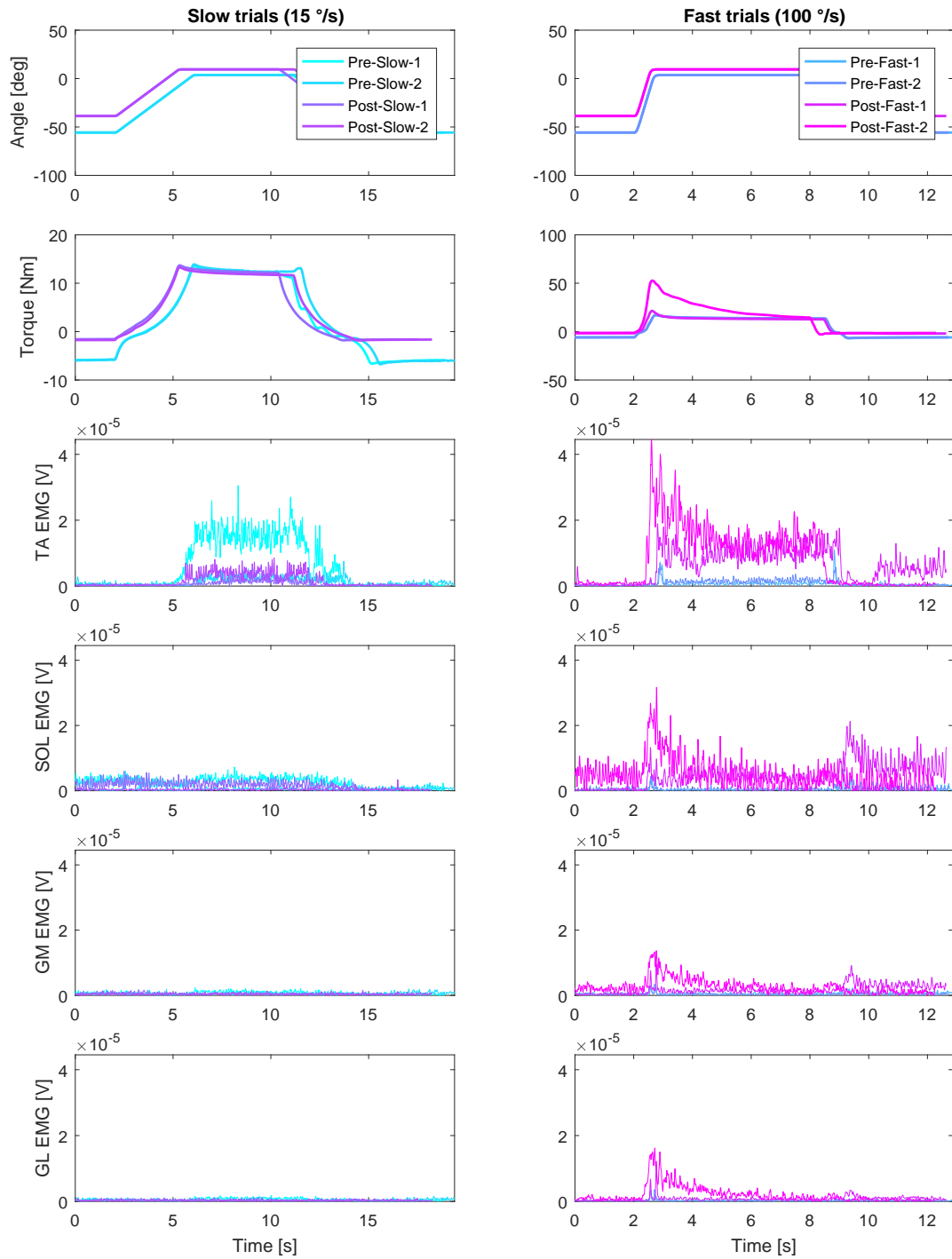


**Figure C.10:** Measured data for Subject 3. From top to bottom: imposed RaH movement profiles, measured joint torque, and muscle EMG from the TA, SOL, GM and GL respectively. Left column: slow trials. Right column: fast trials.

Subject 4

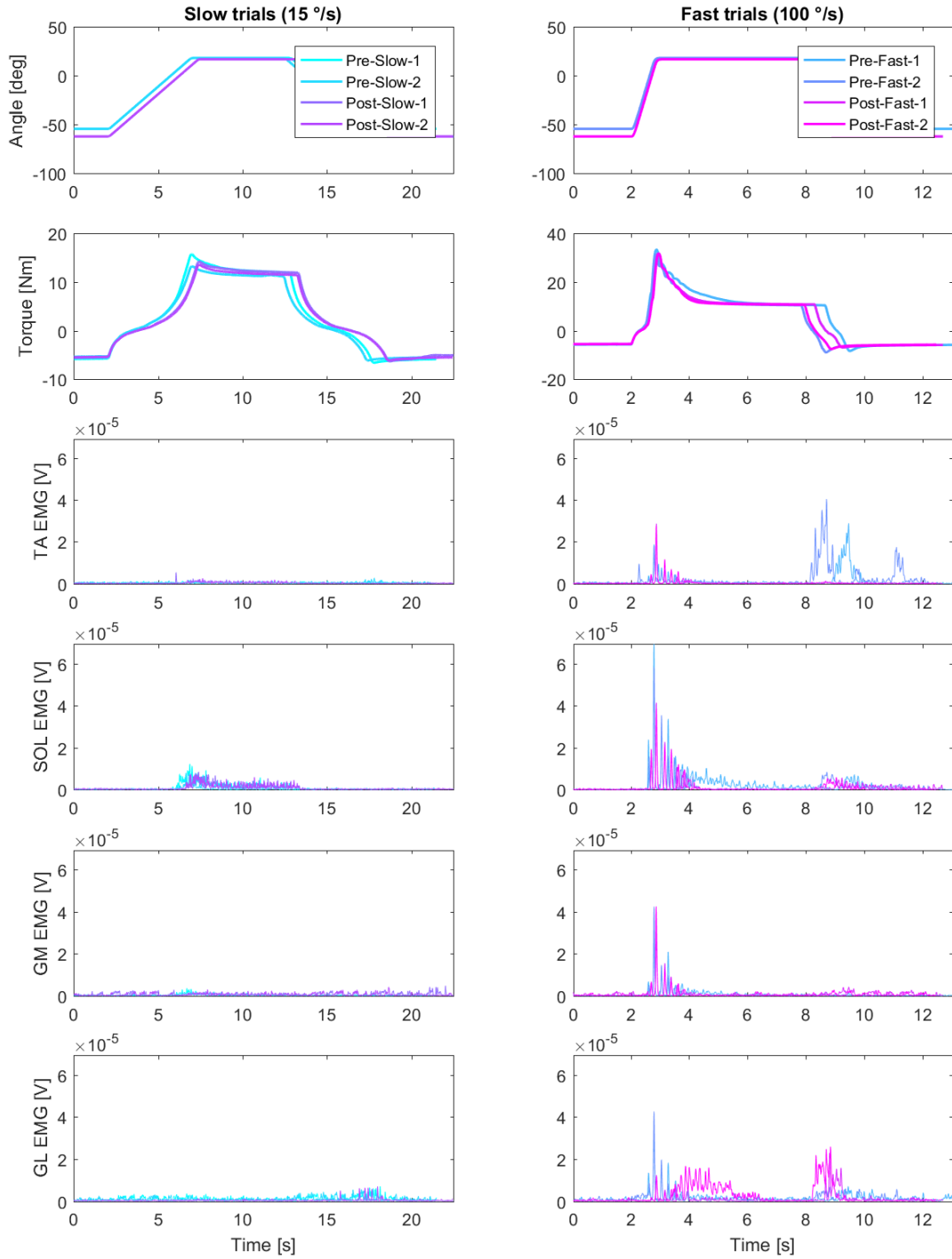


**Figure C.11:** Measured data for Subject 4. From top to bottom: imposed RaH movement profiles, measured joint torque, and muscle EMG from the TA, SOL, GM and GL respectively. Left column: slow trials. Right column: fast trials.

Subject 5

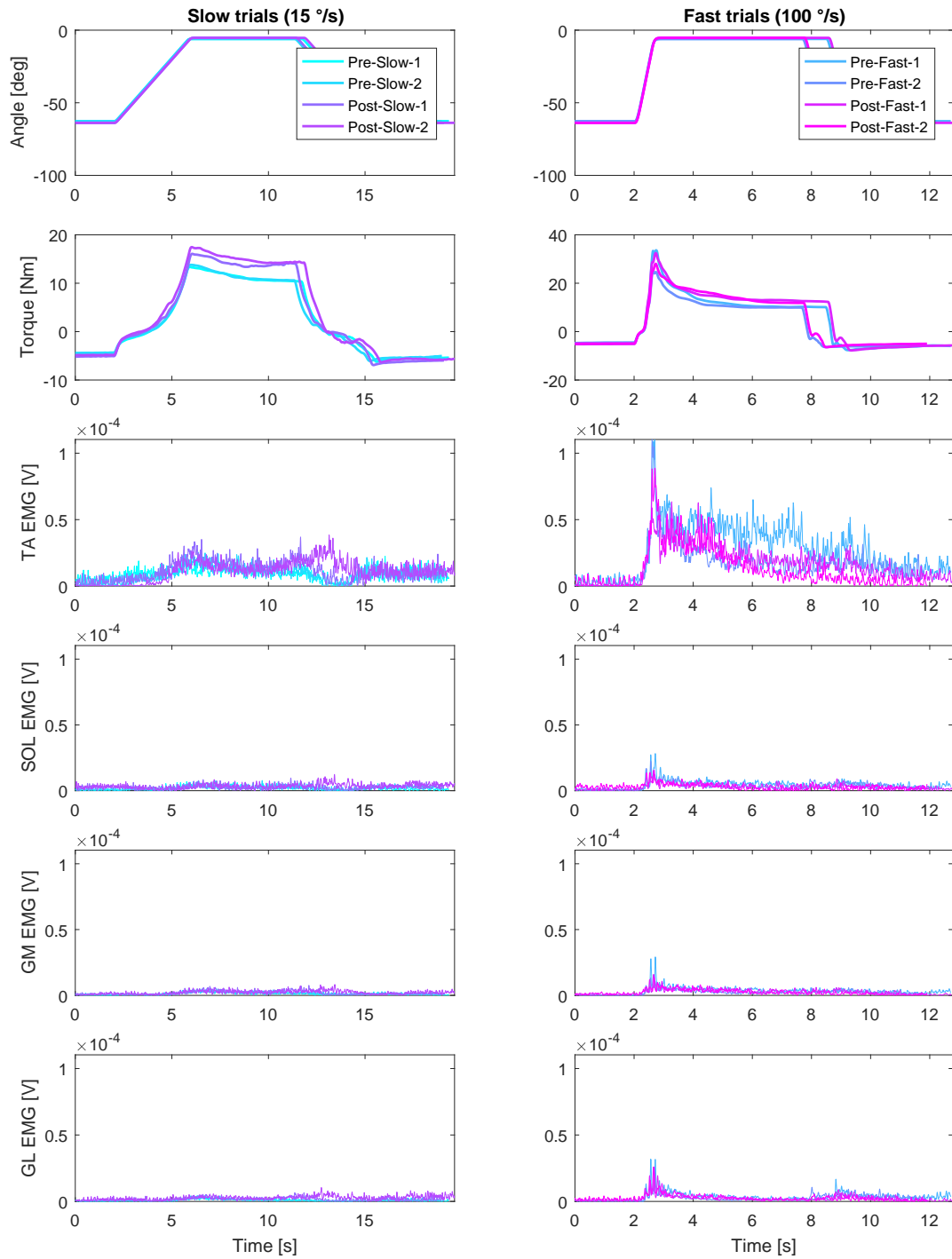


**Figure C.12:** Measured data for Subject 5. From top to bottom: imposed RaH movement profiles, measured joint torque, and muscle EMG from the TA, SOL, GM and GL respectively. Left column: slow trials. Right column: fast trials.

Subject 6

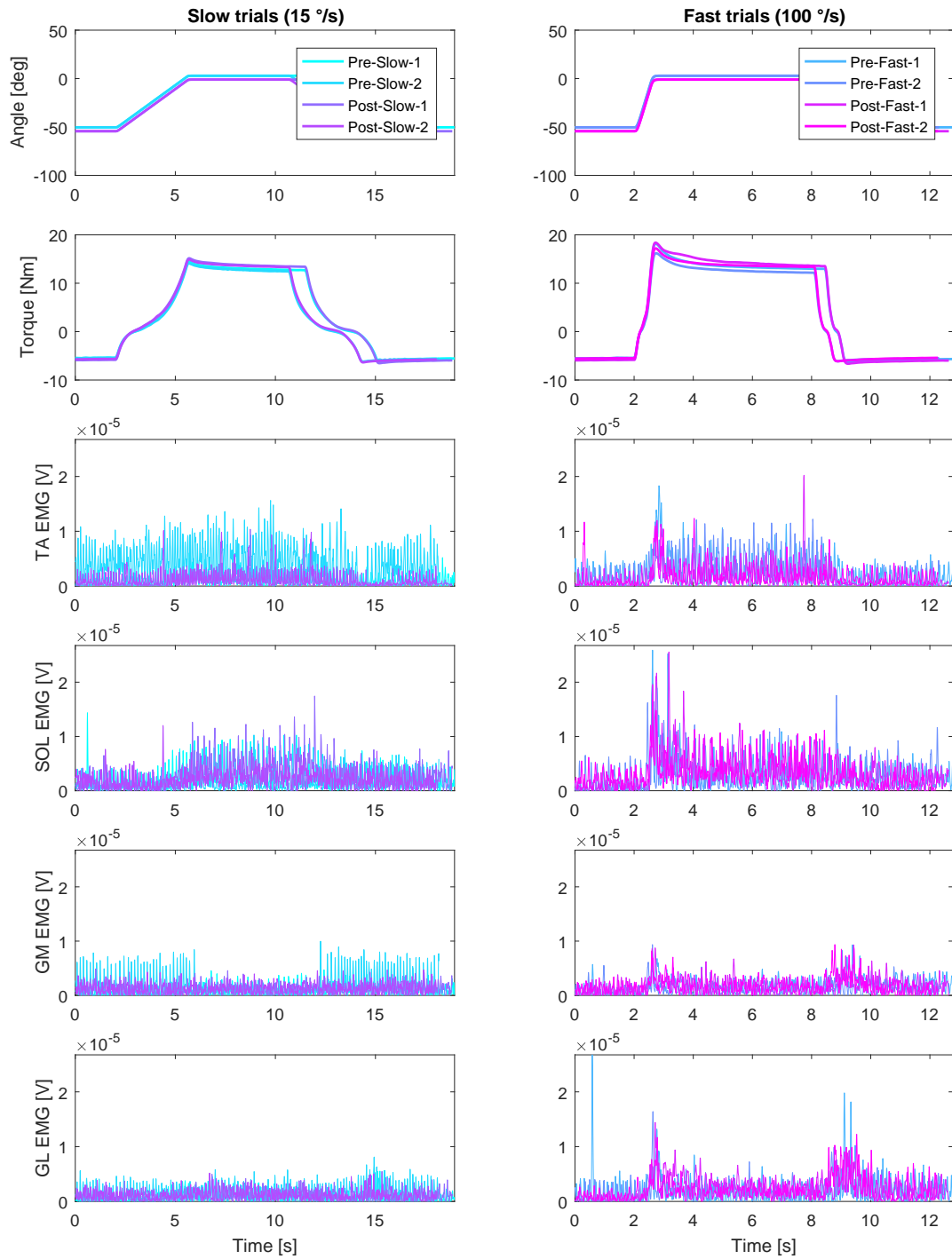


**Figure C.13:** Measured data for Subject 6. From top to bottom: imposed RaH movement profiles, measured joint torque, and muscle EMG from the TA, SOL, GM and GL respectively. Left column: slow trials. Right column: fast trials.

Subject 7

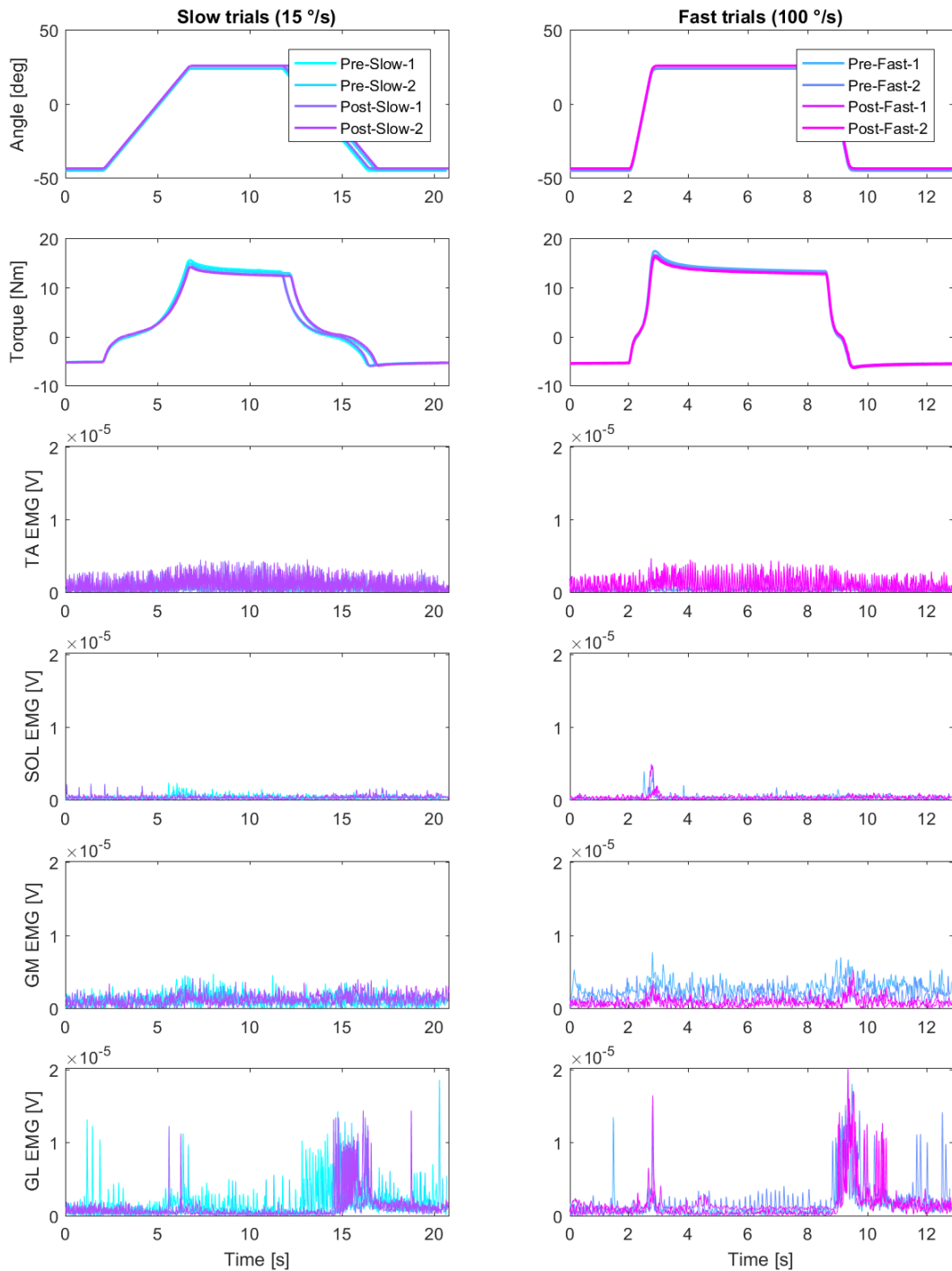


**Figure C.14:** Measured data for Subject 7. From top to bottom: imposed RaH movement profiles, measured joint torque, and muscle EMG from the TA, SOL, GM and GL respectively. Left column: slow trials. Right column: fast trials.

Subject 8

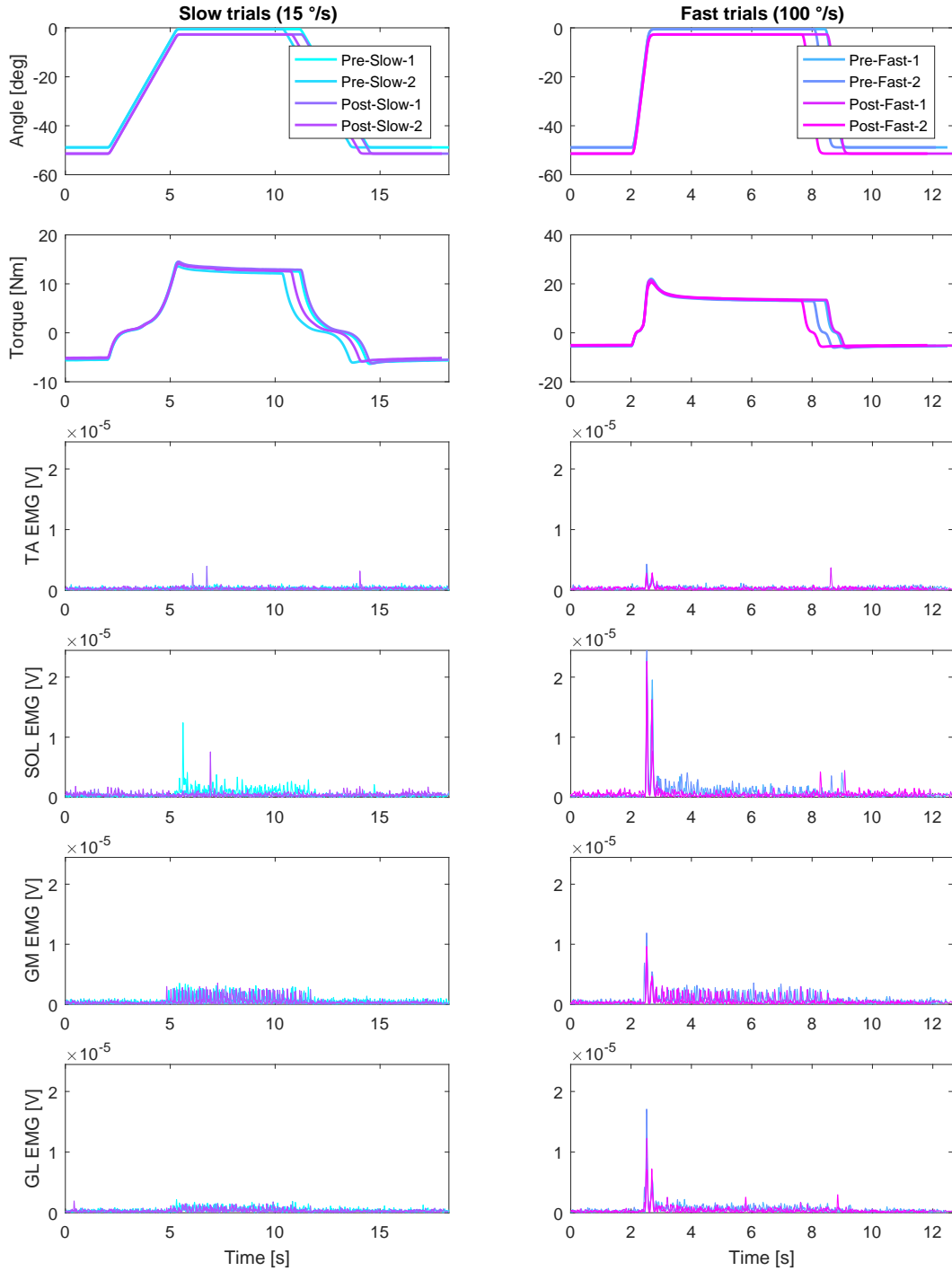


**Figure C.15:** Measured data for Subject 8. From top to bottom: imposed RaH movement profiles, measured joint torque, and muscle EMG from the TA, SOL, GM and GL respectively. Left column: slow trials. Right column: fast trials.

Subject 9

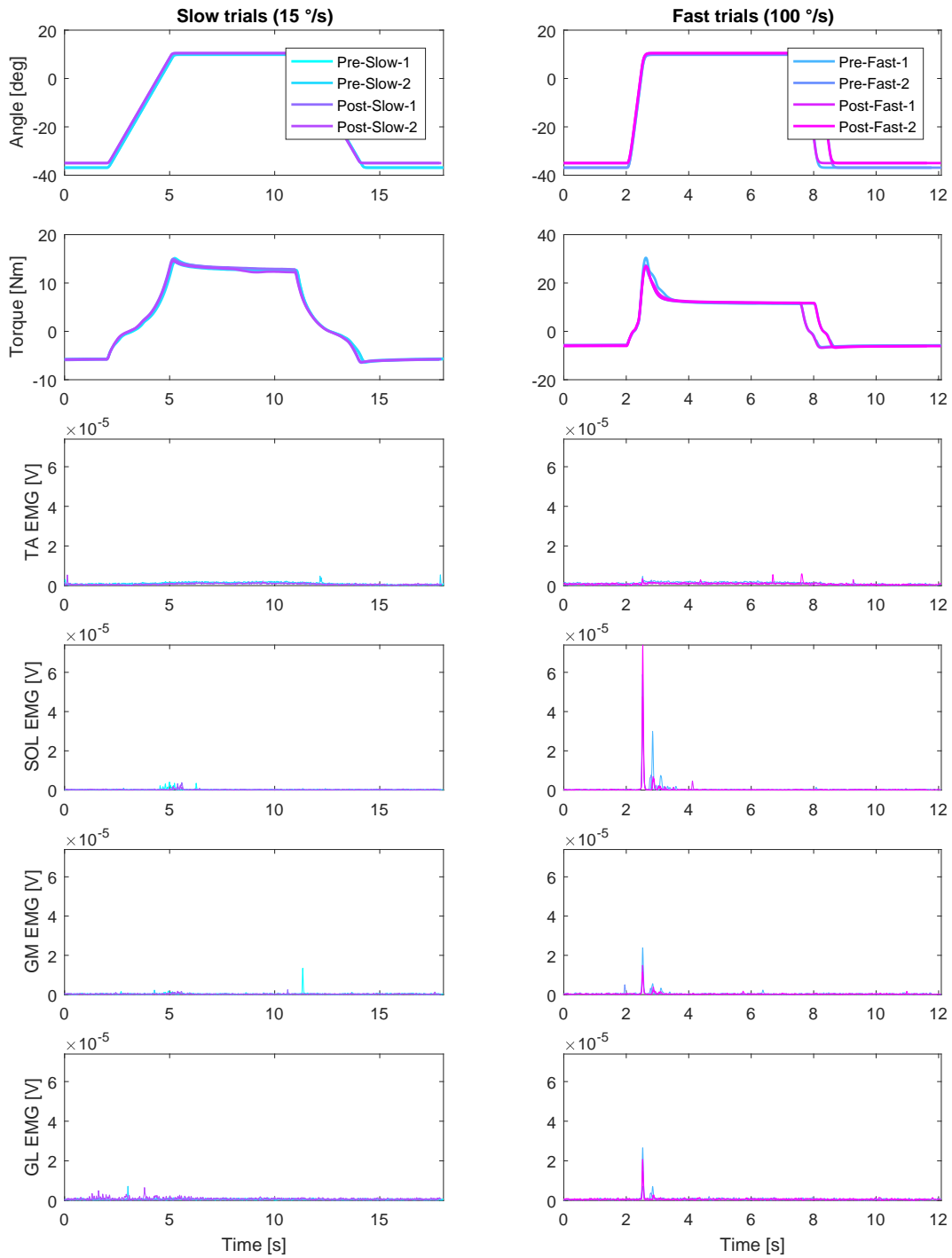


**Figure C.16:** Measured data for Subject 9. From top to bottom: imposed RaH movement profiles, measured joint torque, and muscle EMG from the TA, SOL, GM and GL respectively. Left column: slow trials. Right column: fast trials.

Subject 1

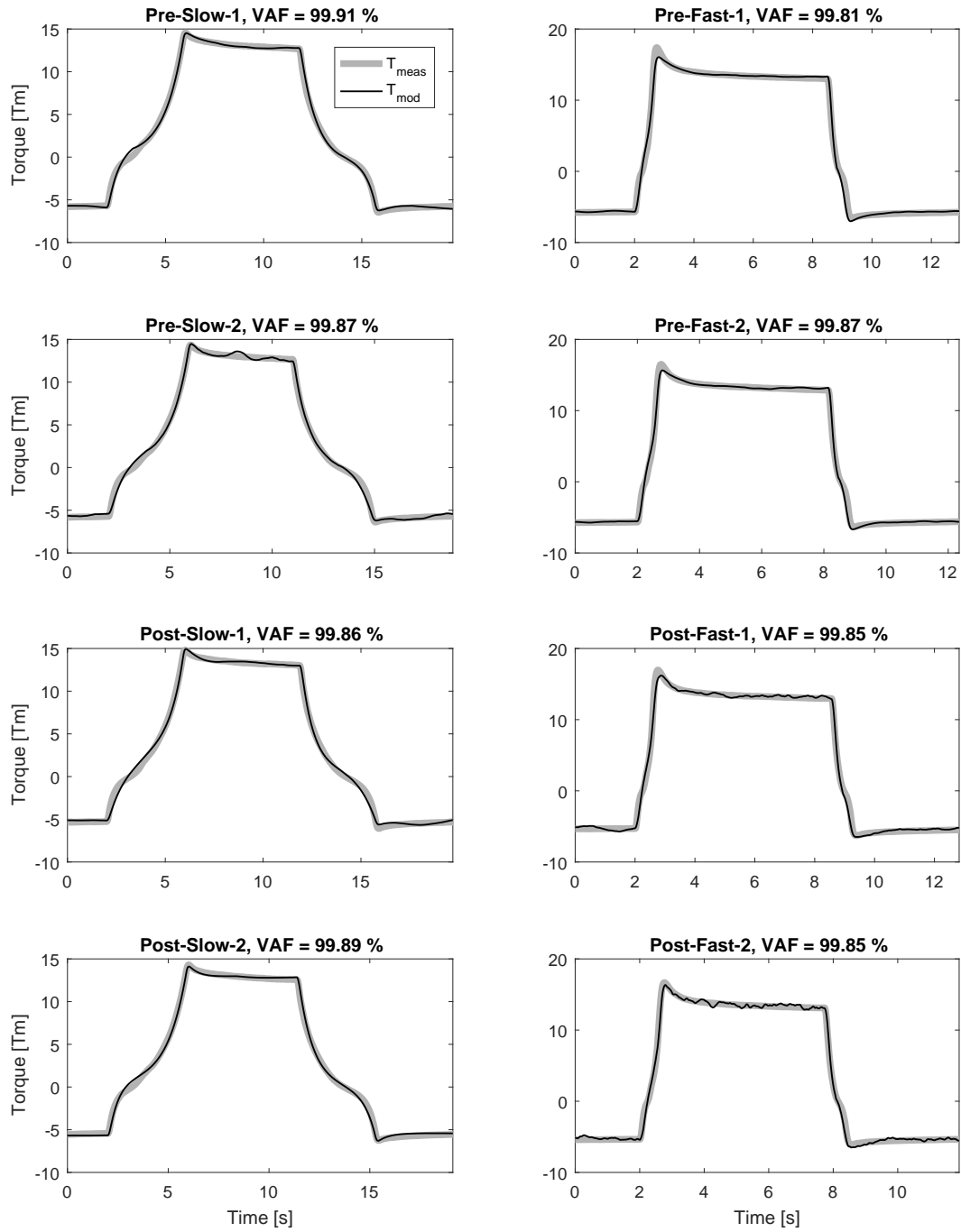


**Figure C.17:** Modeled torque fits for Subject 1. From top to bottom: pre-pre-post-post ESWT treatment. Left column: slow trials. Right column: fast trials.

Subject 2

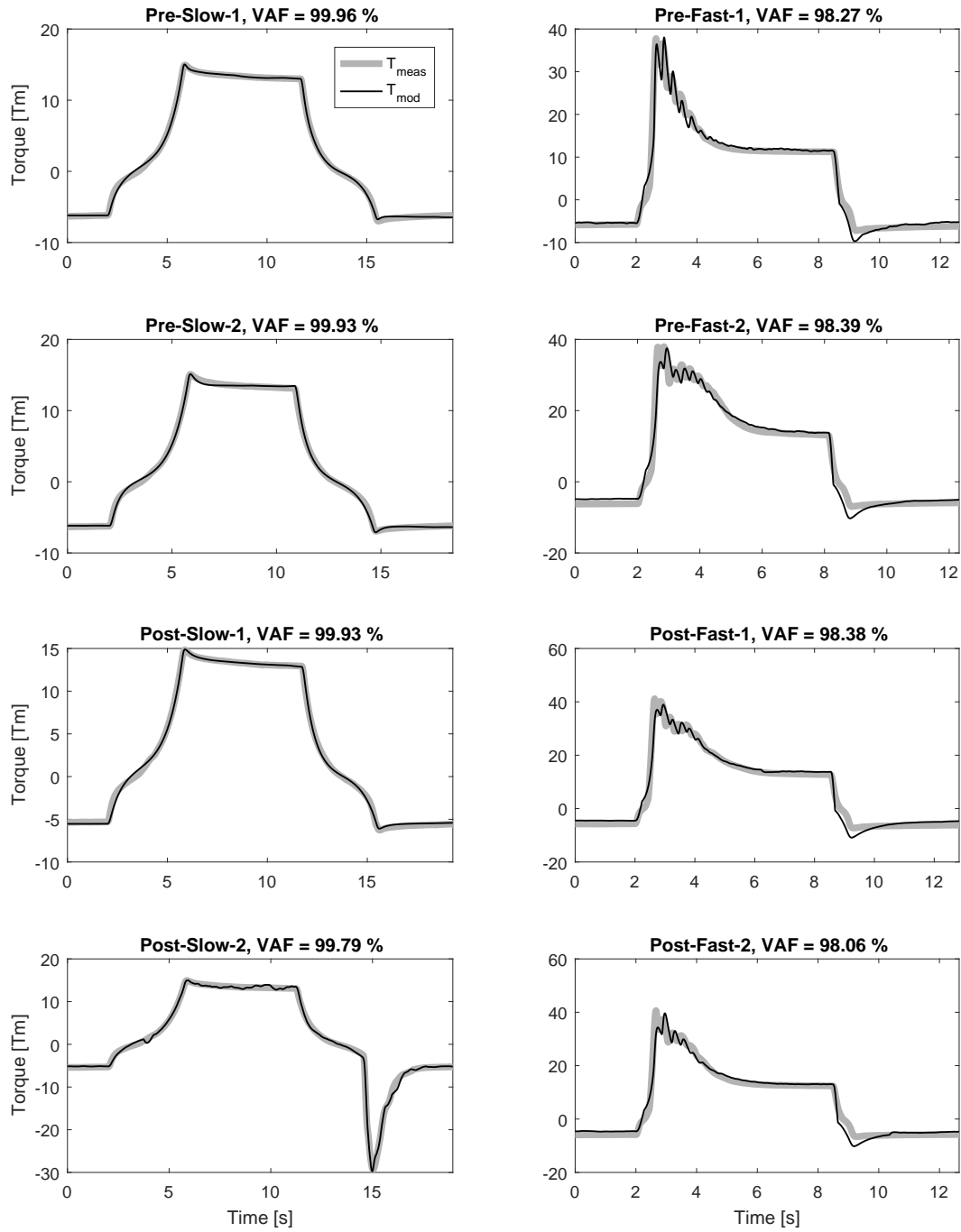


**Figure C.18:** Modeled torque fits for Subject 2. From top to bottom: pre-pre-post-post ESWT treatment. Left column: slow trials. Right column: fast trials.

Subject 3

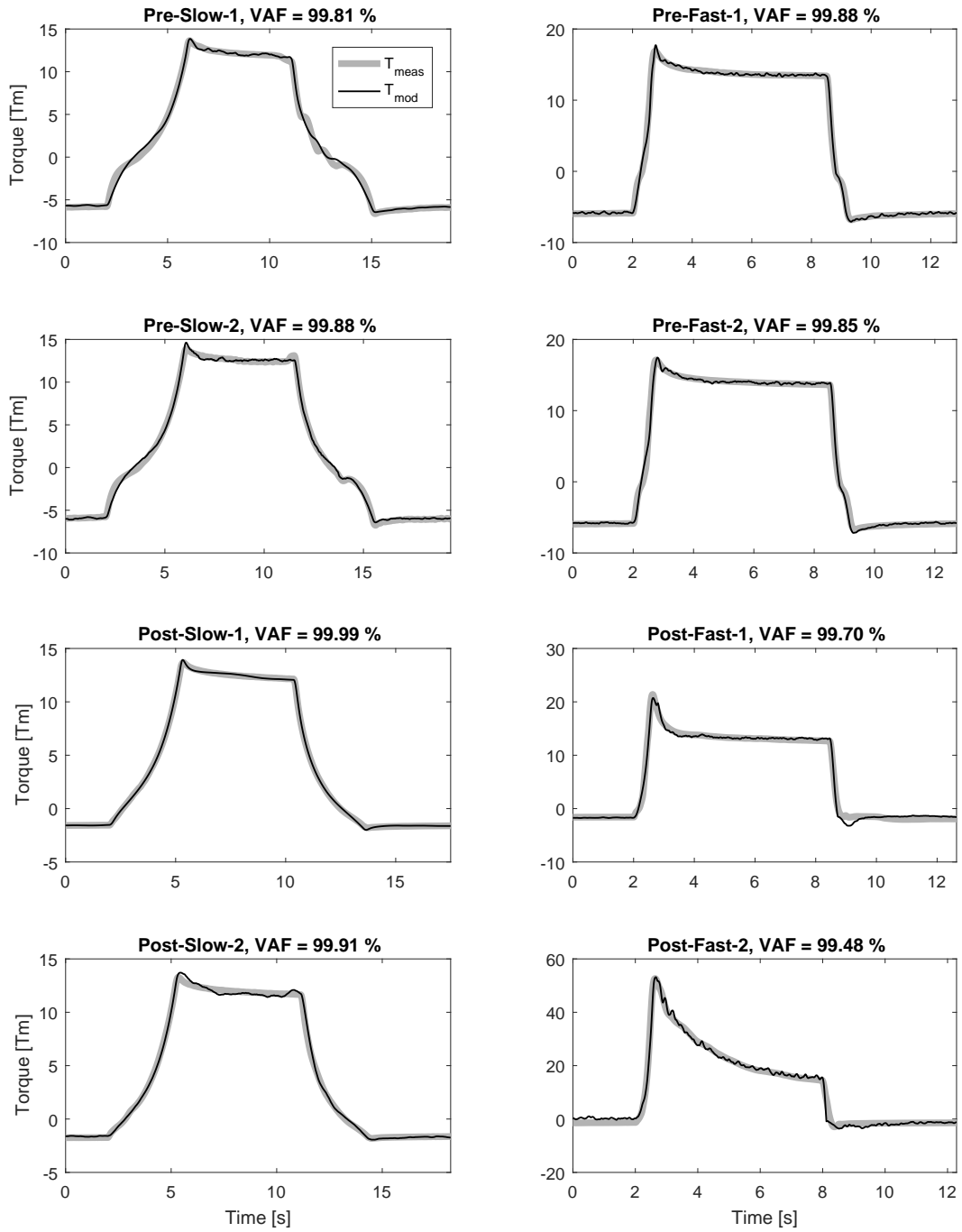


**Figure C.19:** Modeled torque fits for Subject 3. From top to bottom: pre-pre-post-post ESWT treatment. Left column: slow trials. Right column: fast trials.

Subject 4

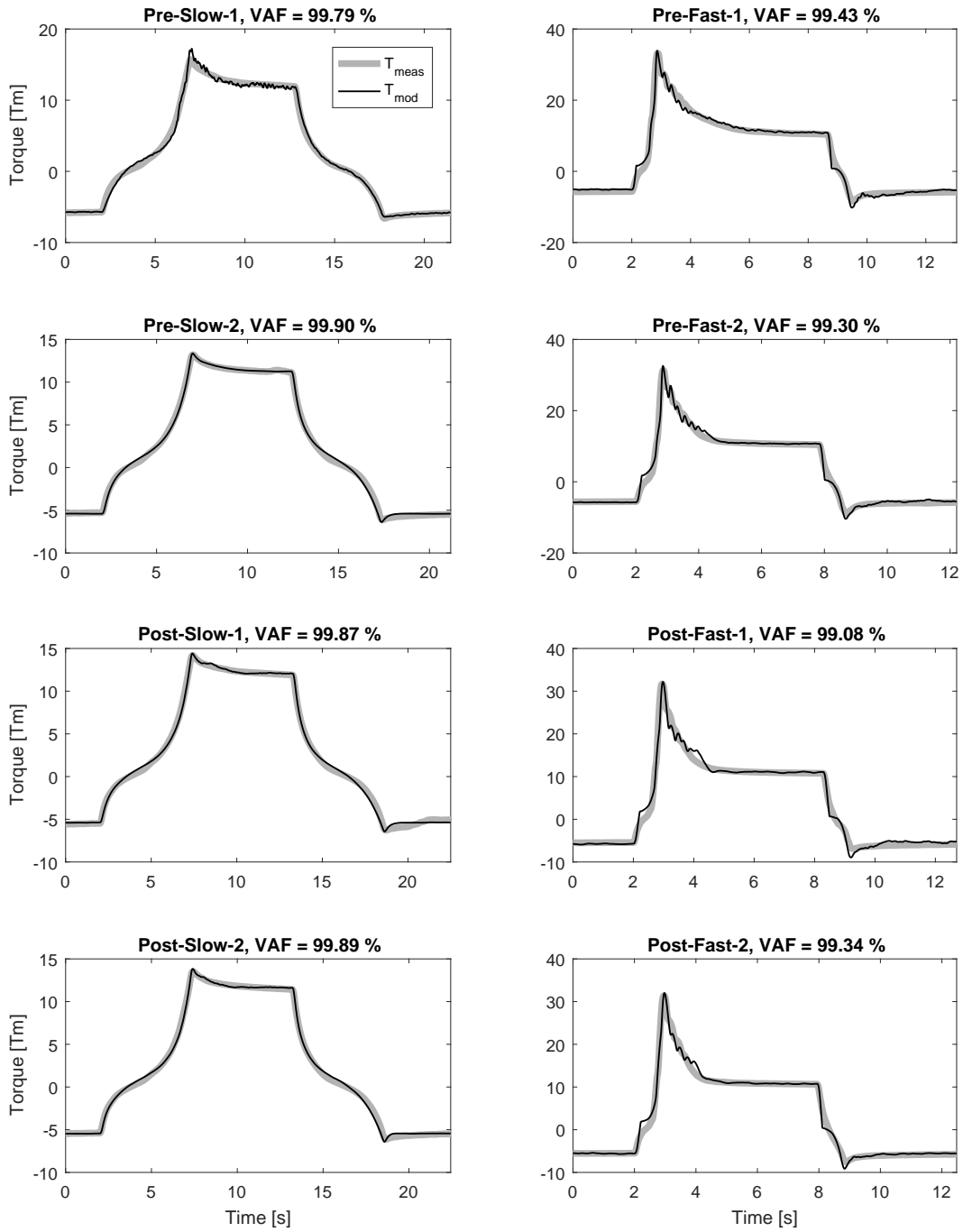


**Figure C.20:** Modeled torque fits for Subject 4. From top to bottom: pre-pre-post-post ESWT treatment. Left column: slow trials. Right column: fast trials.

Subject 5

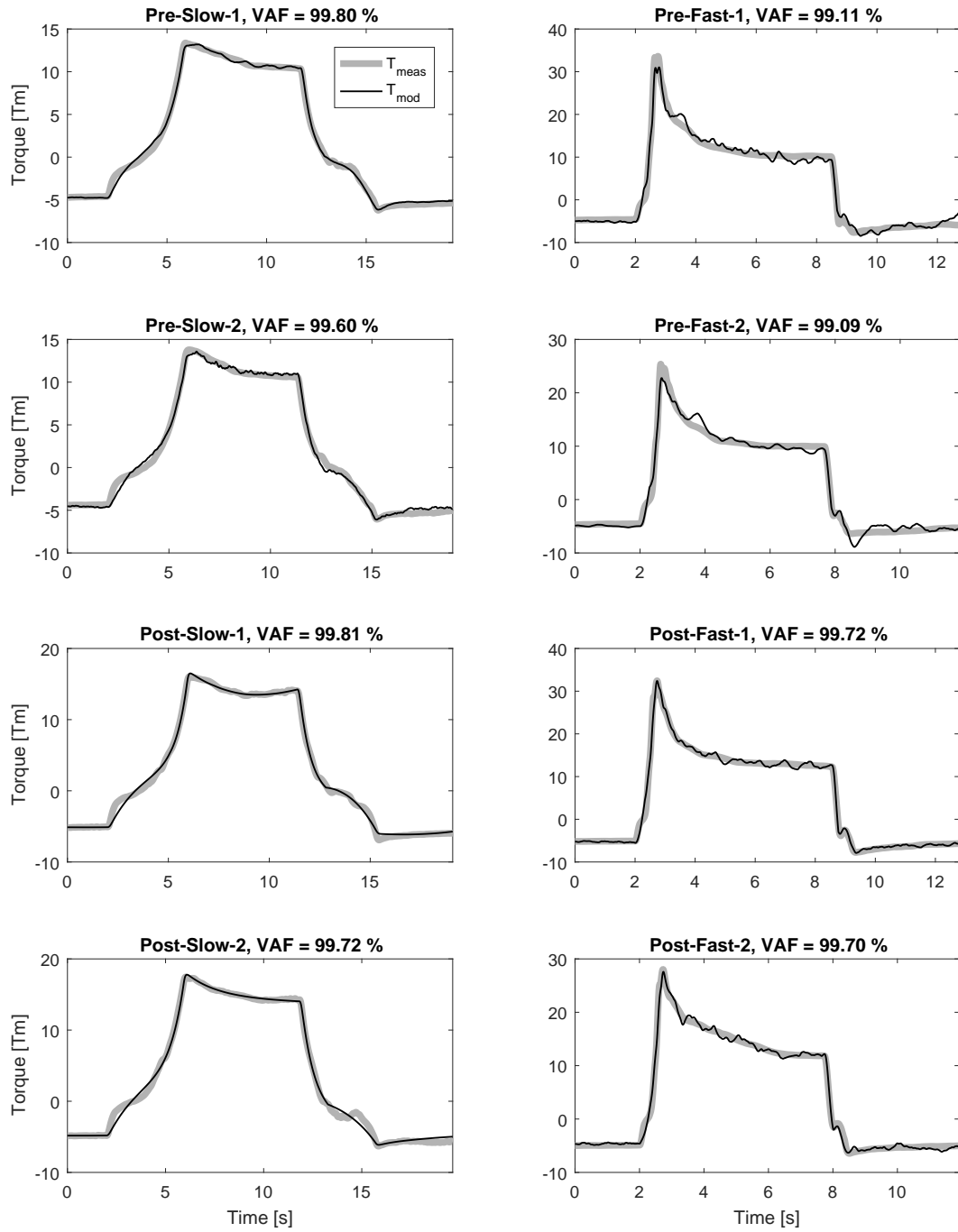


**Figure C.21:** Modeled torque fits for Subject 5. From top to bottom: pre-pre-post-post ESWT treatment. Left column: slow trials. Right column: fast trials.

Subject 6

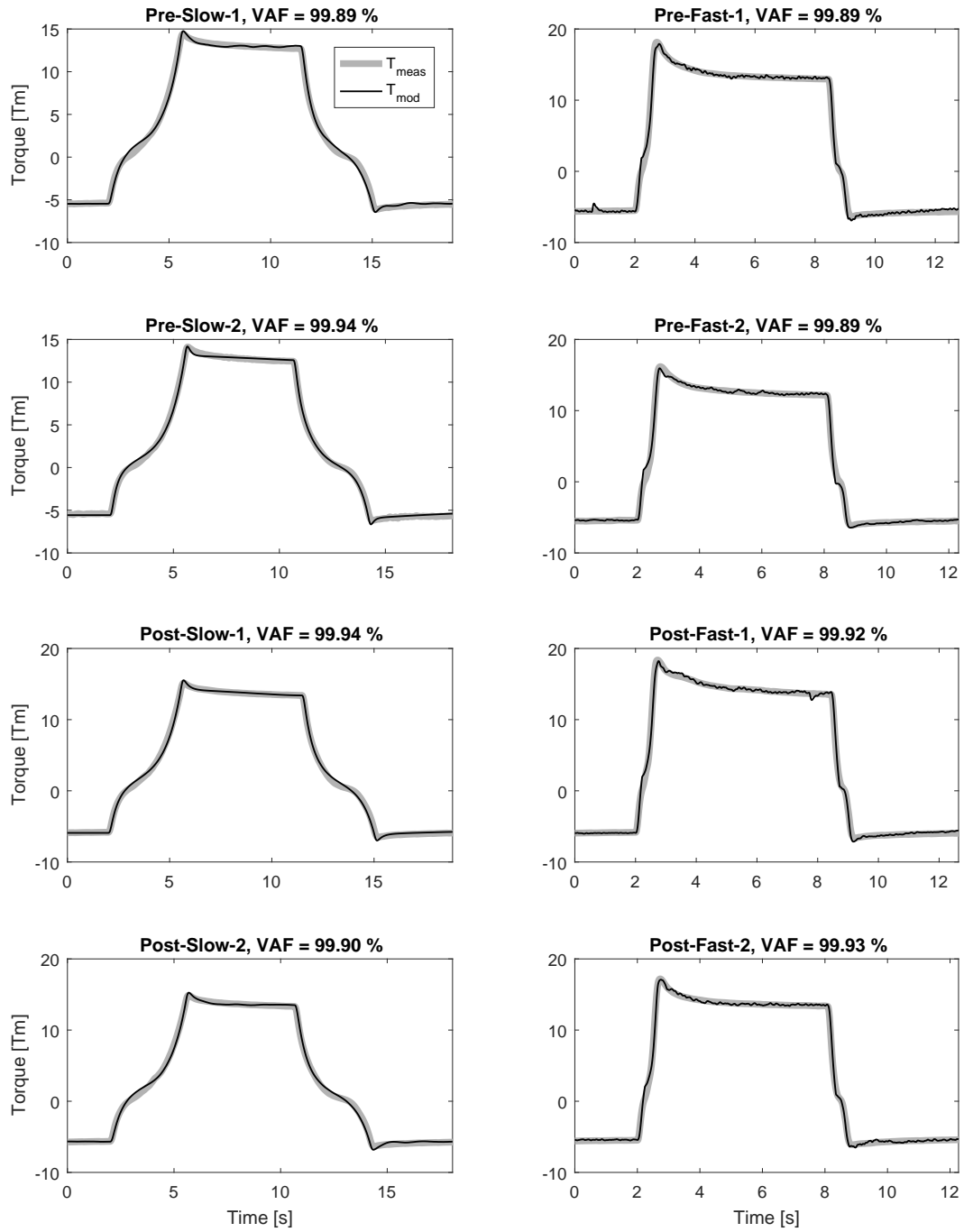


**Figure C.22:** Modeled torque fits for Subject 6. From top to bottom: pre-pre-post-post ESWT treatment. Left column: slow trials. Right column: fast trials.

Subject 7

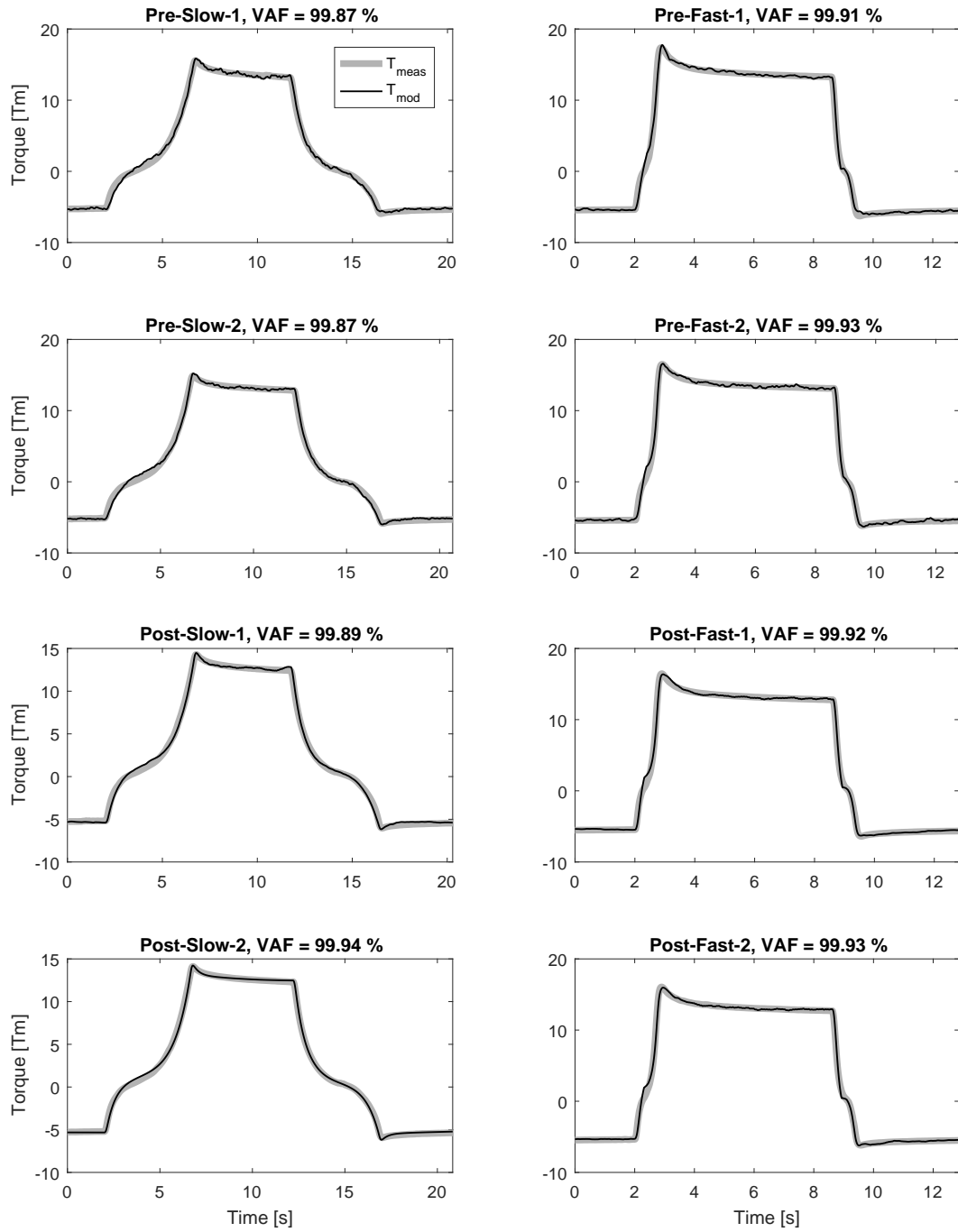


**Figure C.23:** Modeled torque fits for Subject 7. From top to bottom: pre-pre-post-post ESWT treatment. Left column: slow trials. Right column: fast trials.

Subject 8

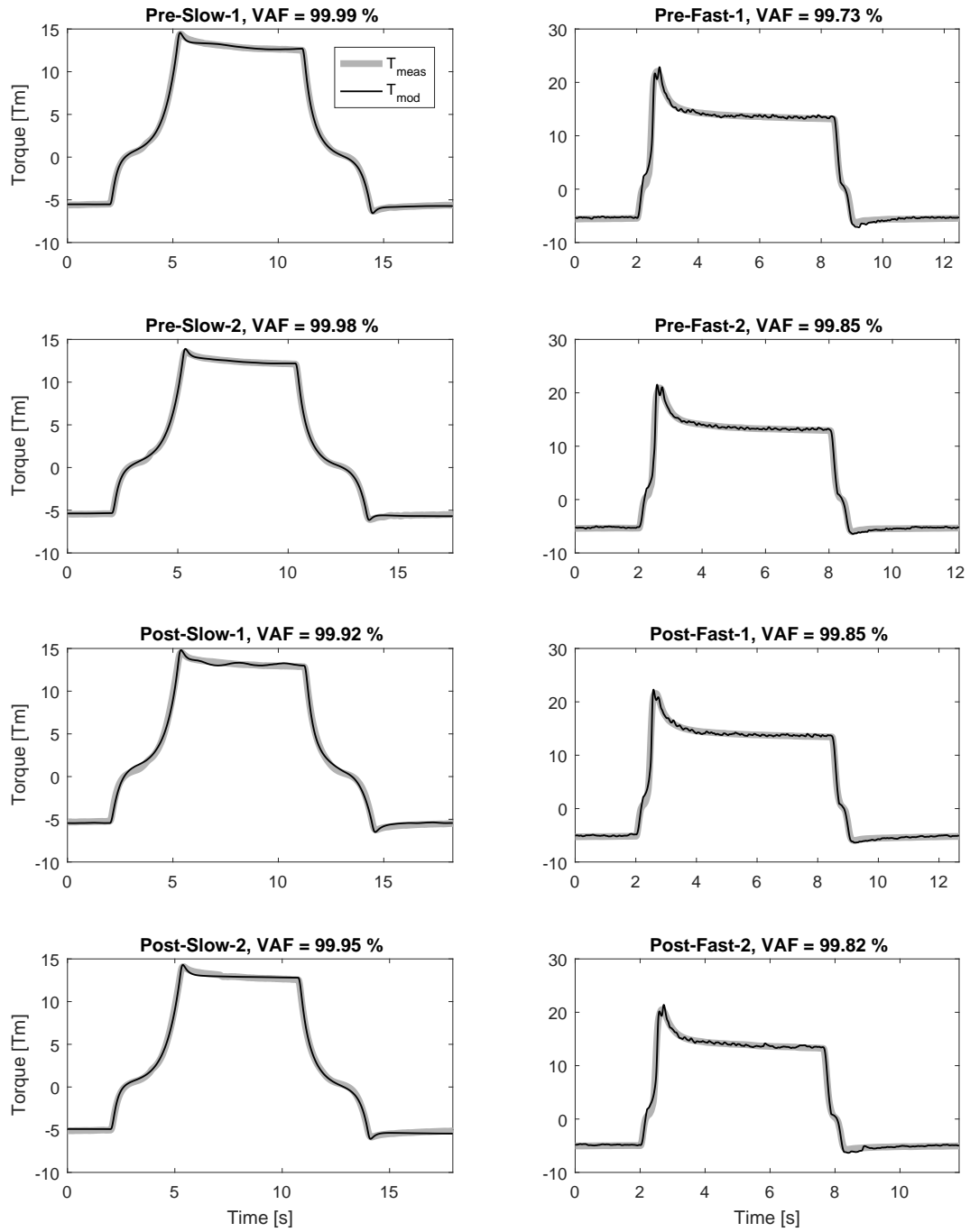


**Figure C.24:** Modeled torque fits for Subject 8. From top to bottom: pre-pre-post-post ESWT treatment. Left column: slow trials. Right column: fast trials.

Subject 9

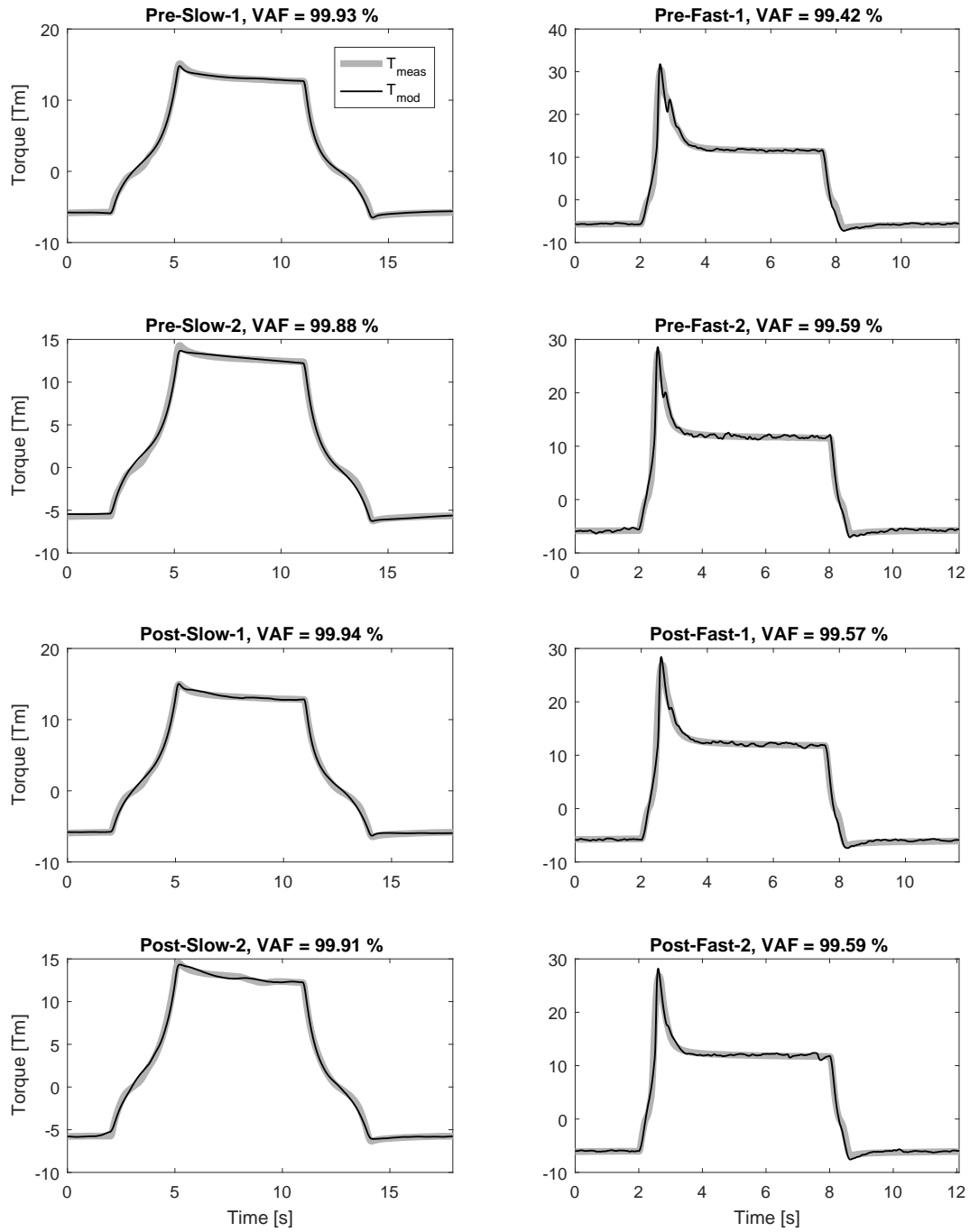


**Figure C.25:** Modeled torque fits for Subject 9. From top to bottom: pre-pre-post-post ESWT treatment. Left column: slow trials. Right column: fast trials.